

## Conformational Refinement of Hydroxamate-Based Histone Deacetylase Inhibitors and Exploration of 3-Piperidin-3-ylindole Analogues of Dacinostat (LAQ824)

Young Shin Cho,<sup>\*,†</sup> Lewis Whitehead,<sup>†</sup> Jianke Li,<sup>†</sup> Christine H.-T. Chen,<sup>†</sup> Lei Jiang,<sup>†</sup> Markus Vögtle,<sup>‡</sup> Eric Francotte,<sup>‡</sup> Paul Richert,<sup>‡</sup> Trixie Wagner,<sup>‡</sup> Martin Traebert,<sup>‡</sup> Qiang Lu,<sup>†</sup> Xueying Cao,<sup>†</sup> Berengere Dumotier,<sup>‡</sup> Jasna Fejzo,<sup>†</sup> Srinivasan Rajan,<sup>†</sup> Ping Wang,<sup>†</sup> Yan Yan-Neale,<sup>†</sup> Wenlin Shao,<sup>†</sup> Peter Atadja,<sup>†</sup> and Michael Shultz<sup>†</sup>

<sup>†</sup>Novartis Institutes for Biomedical Research, 250 Massachusetts Avenue, Cambridge, Massachusetts 02139, and <sup>‡</sup>Werk Klybeck, Klybeckstrasse 141, CH-4002 Basel, Switzerland

Received January 6, 2010

Inspired by natural product HDAC inhibitors, we prepared a series of conformationally restrained HDAC inhibitors based on the hydroxamic acid dacinostat (LAQ824, **7**). Several scaffolds with improved biochemical and cellular potency, as well as attenuated hERG inhibition, were identified, suggesting that the introduction of molecular rigidity is a viable strategy to enhance HDAC binding and mitigate hERG liability. Further SAR studies around a 3-piperidin-3-ylindole moiety resulted in the discovery of compound **30**, for which a unique conformation was speculated to contribute to overcoming increased lipophilicity and attenuating hERG binding. Separation of racemate **30** afforded **32**, the *R* enantiomer, which demonstrated improved potency in both enzyme and cellular assays compared to dacinostat.

Histone acetylation/deacetylation is one of the few enzymatic activities implicated in the unpacking/packing of chromatin and subsequent regulation of gene transcription.<sup>1</sup> Histone deacetylases (HDACs) catalyze the removal of acetyl groups from lysine residues at the N-terminal tails of histones, which results in condensation of chromosomal DNA and transcriptional repression.<sup>2</sup> These enzymes also regulate the acetylation levels of non-histone proteins involved in cell growth and survival pathways such as  $\alpha$ -tubulin, hsp90, and p53.<sup>3</sup> There are four identified classes of HDACs (classes I–IV), which are characterized by their different substrate specificities and subcellular localization.<sup>4</sup> Many research groups are active in elucidating the physiological role of different HDACs in cells, and there has been great effort to develop HDAC inhibitors as novel cancer therapeutics.<sup>5</sup>

Small molecule inhibitors of HDACs have been identified both synthetically and from natural sources, and several inhibitors are at various stages of clinical development. On the basis of their chemical structures, HDAC inhibitors can be divided into several different chemical classes including hydroxamic acids, benzamides, cyclic peptides, and aliphatic acids. The hydroxamic acid vorinostat (SAHA (**1**), Figure 1) is the first HDAC inhibitor approved by the FDA for the treatment of advanced cutaneous T-cell lymphoma (CTCL),<sup>6</sup> and ITF-2357 (**2**) and belinostat (PXD-101 (**3**)) are in phase II clinical trials for the treatment of hematological tumors. Benzamide-based HDAC inhibitors MS-275 (**4**) and MGCD-0103 (**5**) are in phase II clinical trials against a variety of hematological and solid tumors. Naturally occurring HDAC inhibitor romidepsin (FK-228 (**6**)),<sup>7</sup> a bicyclic depsipeptide, has

recently been approved by FDA for treatment of patients with CTCL. Our initial efforts in this area culminated in the discovery of the hydroxamic acid dacinostat (LAQ824, **7**).<sup>8</sup> Herein, we report our strategy to identify analogues with improved potency and safety profiles and progress made in the 3-piperidin-3-ylindole series.

While examining different classes of HDAC inhibitors, we were intrigued by the HDAC inhibitory profile of the natural products such as romidepsin (**6**), spiruchostatin A (**8**), and apicidin (**10**) (Figures 1 and 2). In 2004, Yurek-George and co-workers reported the total synthesis of spiruchostatin A (**8**), a potent HDAC inhibitor that causes the accumulation of acetylated histone-H4.<sup>9</sup> Like romidepsin (**6**),<sup>10</sup> spiruchostatin A is presumed to be reduced intracellularly to release a zinc-binding thiol. Reduced spiruchostatin A is a potent inhibitor of HDAC1 (IC<sub>50</sub> = 0.62 nM) and inhibits the growth of several cancer cell lines with IC<sub>50</sub> values of 1–10 nM. However, *epi*-spiruchostatin A (**9**), prepared by the same group, was inactive in the same cancer cell lines even at 10  $\mu$ M. (*S*)-Stereochemistry at C(1) of spiruchostatin A appears to be critical to garner a favorable interaction between the cyclic depsipeptide “cap” moiety and the amino acid residues around the rim of HDAC1’s binding channel. Such impact of a single stereocenter on potency was also demonstrated during the medicinal chemistry campaigns based on apicidin (**10**). In this case, chirality at C(12) was critical to obtain an optimal spatial relationship between the “cap” and the rest of the molecule, thereby promoting HDAC inhibition.<sup>11</sup> Clearly, these natural product HDAC inhibitors utilize intrinsic conformational constraints to ensure optimal enzyme binding. We recognized several structural similarities between apicidin and our synthetic HDAC inhibitor, dacinostat (**7**), such as indole moieties and zinc-binding carbonyl moieties separated by different spacers. An *in silico* alignment of computationally

<sup>\*</sup>To whom correspondence should be addressed. Phone: 617-871-3495. Fax: 617-871-4081. E-mail: youngshin.cho@novartis.com.

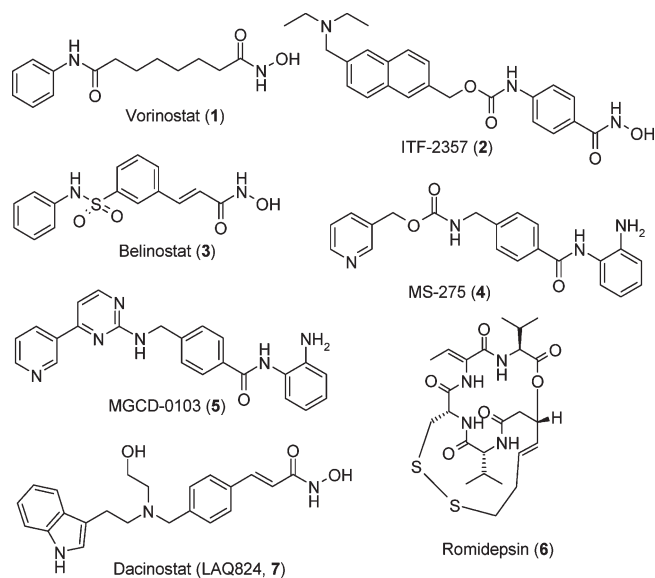


**Figure 1.** Structures of small molecule HDAC inhibitors.

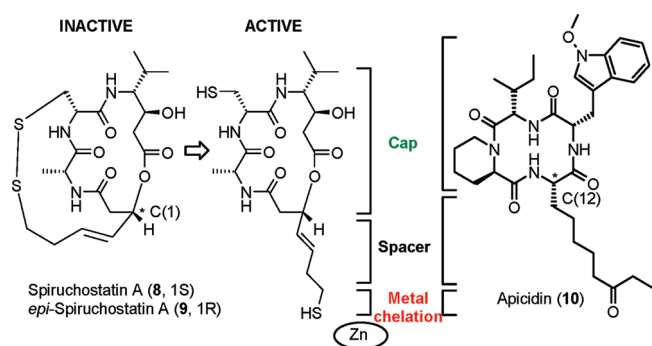


**Figure 2.** Structures of spiruchostatin A (8), *epi*-spiruchostatin A (9), and apicidin (10).

determined dacinostat conformations with a published X-ray crystal structure of apicidin<sup>12</sup> showed good overlap (Figure 3), suggesting that the binding mode of natural product HDAC inhibitors might be mimicked by restraining the conformational flexibility of dacinostat.

To systematically incorporate conformational constraint into dacinostat (7), we generated an HDAC1 homology model based on an in-house HDAC8 X-ray crystal structure.<sup>14</sup> When dacinostat (7) was docked into the HDAC1 enzyme, the “cap” of 7, roughly defined as the aminoalkyl-indole region, was found to interact with the rim of the HDAC binding channel and the hydrophobic surface (Figure 4). The benzene ring of 7 docked in proximity to the three phenyl rings of residues Phe150, Tyr204, and Phe205 to form favorable hydrophobic interactions. This conformation also allowed the protonated benzylamine to contact Asp99 through a salt bridge. The hydroxyethyl unit ( $-\text{CH}_2\text{CH}_2\text{OH}$ ) was found to interact with either the primary or secondary hydration shell of Asp99 and Glu98 and with their methylene groups. The indole moiety was localized above Phe205, providing another hydrophobic contact. This indicated to us that substitutions off the indole ring might be used to explore additional interactions with the HDAC1 hydrophobic surface.

On the basis of this model, we probed the interaction of dacinostat-like analogues with HDACs by introducing different

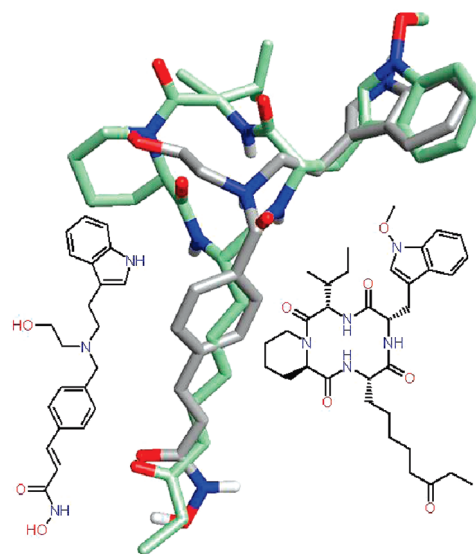


**Figure 3.** Apicidin (10, green) crystal structure superimposed with dacinostat (7, gray) using FieldAlign.<sup>13</sup>

spatial relationships between the indole of the “cap” and the HDAC “channel binder”. To this end, the flexible dacinostat spacer was rigidified (11–18) to access subtle conformational changes in analogue structures (Figure 5). In addition, we expected to improve HDAC1 binding affinity by reducing rotational entropy. For direct comparison among these conformationally constrained analogues, we synthesized a series of compounds, albeit as racemates, with the “cap” fixed as 2-methylindole.

## Chemistry

Compounds 11–13 were assembled from the secondary amines 19–21, which were prepared following procedures outlined in Scheme 1. Reaction of 2-methylindole with *N*-benzyl-3-piperidone under acidic conditions resulted in a regioisomeric mixture of condensation products which was subsequently reduced to piperidinyndole 19 under hydrogenation conditions.<sup>15</sup> 2-Methylindole and maleimide were heated to reflux in glacial acetic acid to provide 2,5-pyrrolidinedione, which was then converted to piperidinyndole 20 via  $\text{LiAlH}_4$  reduction.<sup>16</sup> Synthesis of 21 commenced with the condensation reaction of the magnesium salt of 2-methylindole with the acid chloride of *N*-Boc-2-piperidinecarboxylic acid to afford a 3-ketoindole; these conditions also removed the Boc protecting group. Reduction with  $\text{LiAlH}_4$  gave piperidinylmethylindole 21.<sup>17</sup> The amines 19 and 21 were converted to the final products 11 and 13, respectively, via reductive amination with (*E*)-3-(4-formylphenyl)acrylic acid methyl ester 22 and subsequent conversion of the methyl esters to the hydroxamic acids.<sup>8</sup> Alternatively, compound 12 was prepared via reaction of the amine 20 with 4-bromobenzyl bromide followed by a Heck cross-coupling with methyl acrylate<sup>18</sup> and hydroxamic acid conversion. Synthesis of 14 started with reductive amination between the known compounds (2-methyl-1*H*-indol-3-yl)acetaldehyde 23 and 2-(4-bromophenyl)-pyrrolidine 24 (Scheme 1).<sup>19</sup> Heck reaction followed by treatment of the resulting methyl ester with aqueous hydroxylamine solution in the presence of sodium methoxide provided 14. Syntheses of compounds 15–18 were reported previously.<sup>20</sup>

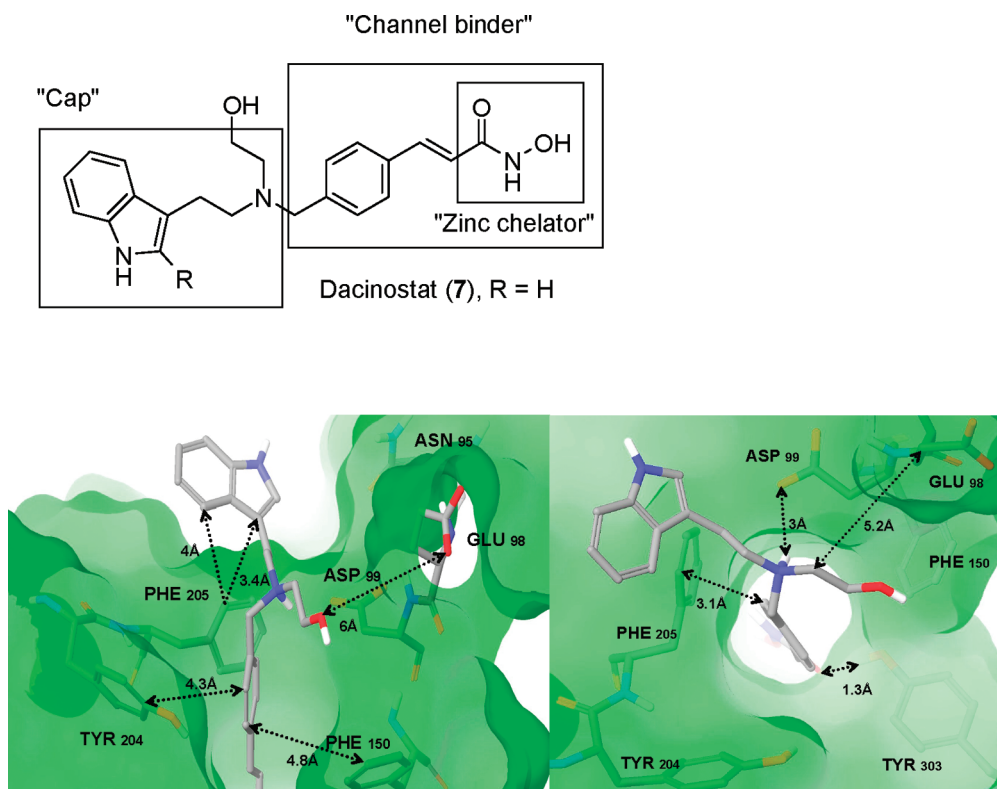


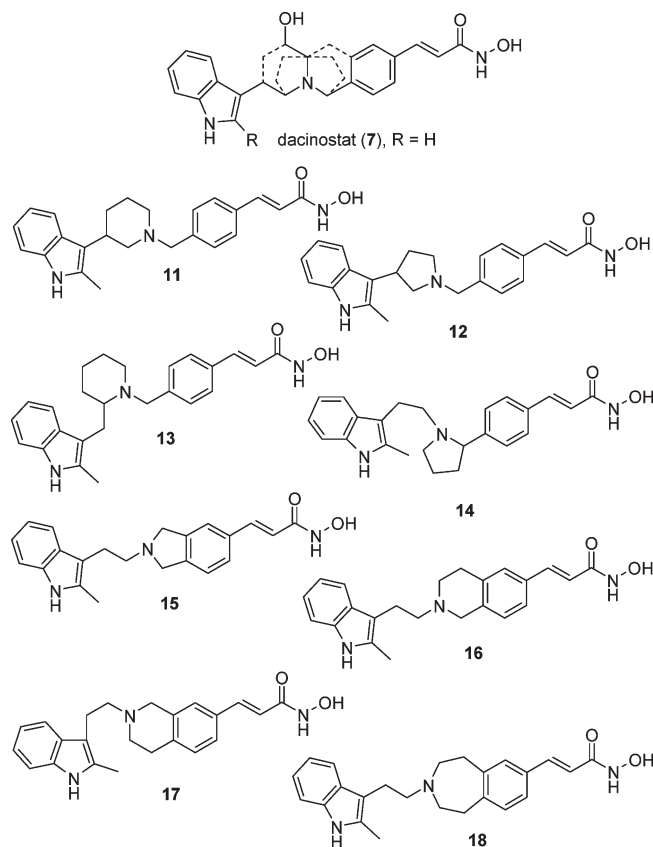
**Figure 4.** Dacinostat (7) docked within an HDAC1 homology model: (left) side view; (right) top view.

## Results and Discussion

The biochemical activity of each compound was assessed using purified HDAC1.<sup>21a</sup> The antiproliferative activity of these compounds was determined in the HCT116 human colon cancer cell line and the H1299 human lung cancer line.<sup>21a</sup> As shown in Table 1, the introduction of conformational restrictions to dacinostat (7) has varying effects on biological activity. 3-Piperidin-3-ylindole **11** and 3-pyrrolidin-3-ylindole **12** demonstrate improved biochemical and cellular potency over dacinostat (7), while 3-piperidin-2-ylmethylin-dole **13** exhibits a slight loss of potency. Enzymatic and cellular activity also improves when the pyrrolidine is shifted further from the indole, as seen in **14**. Compounds **15–18**, in which the amine is fused to the benzene ring, do not display any improvements in potency in the enzymatic or cellular assays.

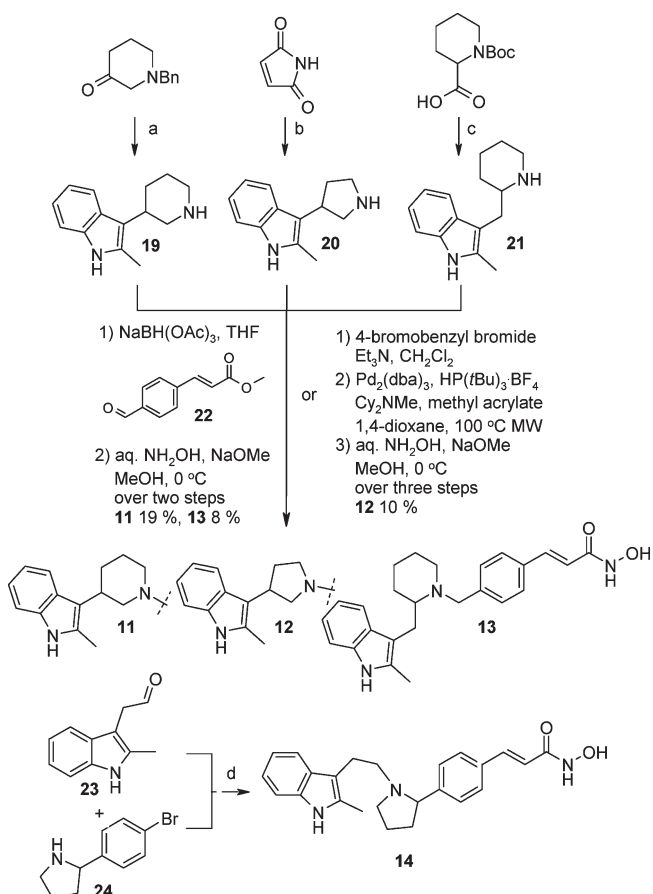
Compounds **11** and **18** were docked in our HDAC1 homology model in an attempt to understand the wide range of in vitro activity observed (Figure 6). We speculate that the improved potency of 3-piperidin-3-ylindole **11** over dacinostat **7** results from the loss of rotational degrees of freedom by rigidifying the linker region while retaining most of the favorable interactions with HDAC1 observed with **7**. The model also suggests that the same key interactions are maintained in docking poses of both *R* and *S* enantiomers, although the *R* enantiomer seems to be more optimal in HDAC binding on visual inspection. On the other hand, **18**, which conformationally locks the amine with the benzene ring, appears to introduce steric hindrance at the edge of the HDAC1 channel. This results in a shift of the benzene ring and loss of directionality of the protonated amine to the Asp99 salt bridge, causing the relative loss in potency.

The presence of a basic tertiary amine and two flanking aromatic rings in this compound series was speculated to be



**Figure 5.** Rigidified analogues.

the potential source of the observed hERG binding.<sup>22</sup> Blockage of the hERG ion channel has been implicated in drug-induced QT interval prolongation, which may lead to

Scheme 1<sup>a</sup>

<sup>a</sup> (a) (1) 2-Methyl-1*H*-indole, aqueous H<sub>3</sub>PO<sub>4</sub>, AcOH, 100 °C, 72%; (2) Pd(OH)<sub>2</sub>/C, H<sub>2</sub>, MeOH, 83%; (b) (1) 2-methyl-1*H*-indole, AcOH, reflux; (2) LAH, THF, 31% over two steps; (c) (1) oxalyl chloride, CH<sub>2</sub>Cl<sub>2</sub>; (2) 2-methyl-1*H*-indole, EtMgBr, benzene; (3) LAH, THF, 15% over three steps; (d) (1) TiCl<sub>4</sub>, NaBH<sub>3</sub>CN, NEt<sub>3</sub>, CH<sub>2</sub>Cl<sub>2</sub>, 50%; (2) Pd<sub>2</sub>(dba)<sub>3</sub>, HP(*t*Bu)<sub>3</sub>BF<sub>4</sub>, methyl acrylate, Cy<sub>2</sub>NMe, dioxane, 97%; (3) aqueous NH<sub>2</sub>OH, NaOMe, MeOH, 0 °C, 65%.

fatal torsades de pointes.<sup>23</sup> Structurally, dacinostat (**7**) satisfies all three key determinants of hERG blockers as described by Farid and co-workers: (1) substituents form extensive ring stacking and/or hydrophobic interactions with the crown-shaped hydrophobic interior of the pore; (2) a basic center interacts with the propeller-shaped hydrophilic field within the pore; (3) the molecule has an ability to assume multiple poses when bound to hERG under the constraints of points 1 and 2.<sup>21b,24</sup> The hERG channel IC<sub>50</sub> values of **11**–**18** were determined in an automated electrophysiology assay (Q-patch clamp assay).<sup>21c</sup> **11** and **14** demonstrated a trend of increasing potency against HDAC and reduced hERG inhibition relative to dacinostat. The difference in hERG inhibitory activity between **7** and **11** cannot be explained by either decreased lipophilicity (cLogP of 2.1 for **7** and 3.8 for **11**) or reduced basicity (measured p*K*<sub>a</sub><sup>21c</sup> of 7.5 for **7** and 7.8 for **11**); therefore, it is plausible that our strategy of introducing rigidity into the dacinostat framework affected the hERG profile by reducing the number of possible binding poses in the hERG channel. Favorable effects of rigidification on HDAC potency and hERG inhibition in several scaffolds prompted us to initiate chemistry efforts to investigate the structure–activity relationships around each constrained spacer, and

**Table 1.** IC<sub>50</sub> Values for Compounds in the HDAC1 Enzyme Assay, HCT116 and H1299 Cellular Assays, and the Patch Clamp Assay<sup>a</sup>

	IC <sub>50</sub> (nM)			
	HDAC1 <sup>b</sup>	HCT116 <sup>c</sup>	H1299 <sup>c</sup>	Q-patch clamp <sup>d</sup>
<b>7</b>	9.0 ± 1.4	13 ± 2	161 ± 7	12200
<b>11</b>	5.0 ± 1.2	5.6	31 ± 1	27600
<b>12</b>	2.8 ± 0.4	3.2	14 ± 10	13400
<b>13</b>	24 ± 1	27 ± 1	153 ± 1	9100
<b>14</b>	3 ± 0	1	4.3 ± 0.7	19400
<b>15</b>	27 ± 4	41 ± 12	232 ± 127	4800
<b>16</b>	41 ± 1	119 ± 18	725 ± 52	14800
<b>17</b>	13 ± 1	42 ± 1	165 ± 13	2700
<b>18</b>	76 ± 4	545 ± 25	> 1,000	3200

<sup>a</sup> See Experimental Section and Supporting Information for detailed descriptions of each assay. <sup>b</sup> Results expressed as the mean ± standard deviation of two to five separate IC<sub>50</sub> determinations. For each determination, a single concentration–inhibition curve was obtained to afford an IC<sub>50</sub> value. <sup>c</sup> Results expressed as the mean ± standard deviation of two separate IC<sub>50</sub> determinations. For each determination, concentration–inhibition curves were obtained in triplicate and then averaged to afford a single IC<sub>50</sub> curve with a ≥95% confidence interval. <sup>d</sup> Results are from single IC<sub>50</sub> determination. For each determination, concentration–inhibition curves were obtained in triplicate and then averaged to afford a single IC<sub>50</sub> curve with a ≥95% confidence interval.

those results will be reported in due course. Herein, we focus our discussion on the 3-piperidin-3-ylindole series based on **11**.

Several analogues of **11** were prepared to understand the effect of substitution on the C(2) position of the indole.<sup>21a</sup> Biochemical and cell viability assay results suggest that a hydrophobic substituent at C(2) is required to improve potency (Table 2);<sup>8,25</sup> however, the increasing lipophilicity also increases hERG inhibition. At this juncture, we introduced a fluorine substituent on the benzene ring in an attempt to modulate the basicity and/or molecular conformation, thereby attenuating the hERG affinity.<sup>26</sup> Despite reduced p*K*<sub>a</sub> values, the incorporation of fluorine resulted in enhanced hERG inhibitory activity in all analogues of the 3-piperidin-3-ylindole series, with the exception of compound **30** (Table 3). This suggests that increased lipophilicity resulting from fluorine substitution may have a dominant role in controlling hERG activity in this series. Compounds **28** and **29** display increased hERG inhibition as well as loss of potency in HDAC enzyme and cellular assays compared to the non-fluorinated analogues **25** and **26**, respectively. Interestingly, compound **30** exhibits about a 2-fold reduction in hERG inhibition compared to **27**; however, we also observe a 3-fold decrease in HDAC enzyme and cell antiproliferation activity. Addition of chlorine instead of fluorine results in more potent hERG inhibition, as illustrated by **31**. We surmised that unique conformational constraints in **30** might be the origin of its reduced hERG affinity, and therefore, we performed density functional calculations on the truncated structure of **30** (Figure 7a).<sup>27</sup> The ortho-fluoro substituent in **30** is proposed to be in proximity to the protonated benzylic amine and methylene hydrogens on the piperidine (X = 1.7 Å, Y = 2.6 Å, respectively). This conformation creates a steric shield around the protonated benzylic amine, which may mitigate external influence, such as solvent or the hERG channel's preferred region for accommodating a cationic center. To test our hypothesis, NMR experiments (<sup>19</sup>F/<sup>1</sup>H 2D HOSEY) with the hydrogen chloride salt of compound **30** in DMSO-*d*<sub>6</sub> were performed (Figure 7b).<sup>21c</sup> Indeed, we observed spatial proximity of the fluorine and several hydrogens predicted by the model.<sup>21d</sup>

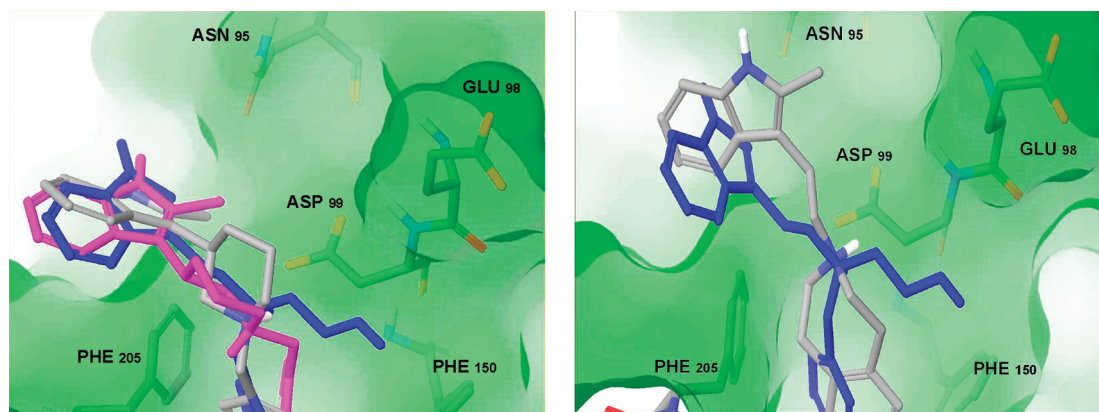


**Figure 6.** Compounds **11** (gray *R*, pink *S*) and **18** (gray) aligned with dacinostat (**7**, blue) in an HDAC1 homology model.

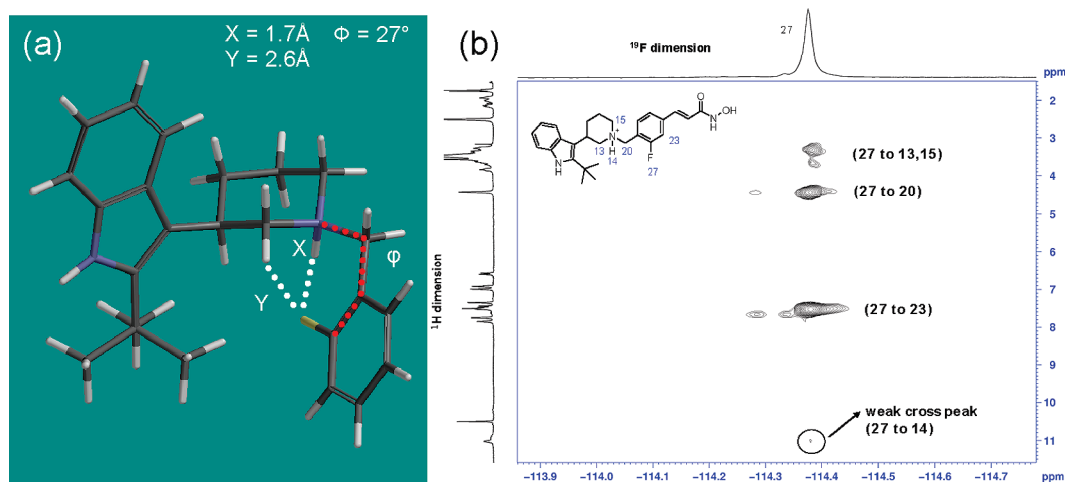


**Figure 7.** (a) Density functional minimized geometries of **30**. *N*-Hydroxyacrylamide functional group was removed to facilitate in silico calculation. (b) Observed "through-space" cross-peaks from the single  $^{19}\text{F}$  atom in compound **30** to the certain protons (13, 14, 15, 20, and 23) in the  $^{19}\text{F}/^1\text{H}$  2D HOSEY NMR spectrum.

**Table 2.**  $\text{IC}_{50}$  Values for Compounds in the HDAC1 Enzyme Assay, HCT116 and H1299 Cellular Assays, and the Patch Clamp Assay,  $\text{pK}_a$  of the Benzylic Amine, $^{21c}$  and  $\text{cLogP}^a$

	R	$\text{IC}_{50}$ (nM)				$\text{pK}_a$	$\text{cLogP}$
		HDAC1 <sup>b</sup>	HCT 116 <sup>c</sup>	H 1299 <sup>c</sup>	Q-patch clamp <sup>d</sup>		
<b>25</b>	H	11 ± 2	25 ± 10	141 ± 74	29300	7.3	3.3
<b>11</b>	Me	5.0 ± 1.2	5.6	31 ± 1	27600	7.8	3.8
<b>26</b>	Ph	11 ± 3	6.9 ± 1.1	31 ± 1	28400	7.7	5.1
<b>27</b>	<sup>t</sup> Bu	3.0 ± 1.4	0.9	6.3 ± 1	13500	7.8	5.1

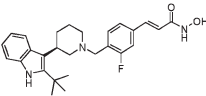
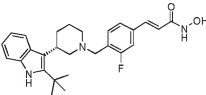
<sup>a</sup> See Experimental Section and Supporting Information for detailed descriptions of each assay. <sup>b</sup> Results expressed as the mean ± standard deviation of two to five separate  $\text{IC}_{50}$  determinations. For each determination, a single concentration–inhibition curve was obtained to afford an  $\text{IC}_{50}$  value. <sup>c</sup> Results expressed as the mean ± standard deviation of two separate  $\text{IC}_{50}$  determinations. For each determination, concentration–inhibition curves were obtained in triplicate and then averaged to afford a single  $\text{IC}_{50}$  curve with a ≥95% confidence interval. <sup>d</sup> Results are from single  $\text{IC}_{50}$  determination. For each determination, concentration–inhibition curves were obtained in triplicate and then averaged to afford a single  $\text{IC}_{50}$  curve with a ≥95% confidence interval.

**Table 3.**  $\text{IC}_{50}$  Values for Compounds in the HDAC1 Enzyme Assay, HCT116 and H1299 Cellular Assays, and the Patch Clamp Assay,  $\text{pK}_a$  of the Benzylic Amine, $^{21c}$  and  $\text{cLogP}^a$

R, X	$\text{IC}_{50}$ (nM)				$\text{pK}_a$	$\text{cLogP}$
	HDAC1 <sup>b</sup>	HCT 116 <sup>c</sup>	H 1299 <sup>c</sup>	Q-patch clamp <sup>d</sup>		
<b>28</b> H, F	136 ± 31	332 ± 82	3520	15300	nd <sup>e</sup>	3.5
<b>29</b> Ph, F	16 ± 1	11 ± 1	106 ± 26	19300	7.4	5.3
<b>30</b> <sup>t</sup> Bu, F	10 ± 1	3.8	20 ± 5	30000	7.3	5.2
<b>31</b> <sup>t</sup> Bu, Cl	19 ± 5	5.2 ± 1.0	60 ± 20	9900	7.4	5.8

<sup>a</sup> See Experimental Section and Supporting Information for detailed descriptions of each assay. <sup>b</sup> Results expressed as the mean ± standard deviation of two to five separate  $\text{IC}_{50}$  determinations. For each determination, a single concentration–inhibition curve was obtained to afford an  $\text{IC}_{50}$  value. <sup>c</sup> Results expressed as the mean ± standard deviation of two separate  $\text{IC}_{50}$  determinations. For each determination, concentration–inhibition curves were obtained in triplicate and then averaged to afford a single  $\text{IC}_{50}$  curve with a ≥95% confidence interval. <sup>d</sup> Results are from single  $\text{IC}_{50}$  determination. For each determination, concentration–inhibition curves were obtained in triplicate and then averaged to afford a single  $\text{IC}_{50}$  curve with a ≥95% confidence interval. <sup>e</sup> nd: not determined.

**Table 4.** IC<sub>50</sub> Values for Compounds in the HDAC1 Enzyme Assay and in the HCT116 and H1299 Cellular Assays and % Inhibition in the Manual Patch Clamp Assay<sup>a</sup>

	Structure	HDAC1 IC <sub>50</sub> (nM) <sup>b</sup>	HCT 116 IC <sub>50</sub> (nM) <sup>c</sup>	H 1299 IC <sub>50</sub> (nM) <sup>c</sup>	Manual Patch Clamp %inhibition @ 30 μM <sup>d</sup>
32		7.5 ± 0.7	0.8 ± 0.3	5.4 ± 0.3	48 ± 6 %
33		15 ± 4	143 ± 64	443 ± 316	70 ± 5 %

<sup>a</sup> See Experimental Section and Supporting Information for detailed descriptions of each assay. <sup>b</sup> Results expressed as the mean ± standard deviation of two to five separate IC<sub>50</sub> determinations. For each determination, a single concentration–inhibition curve was obtained to afford an IC<sub>50</sub> value. <sup>c</sup> Results expressed as the mean ± standard deviation of two separate IC<sub>50</sub> determinations. For each determination, concentration–inhibition curves were obtained in triplicate and then averaged to afford a single IC<sub>50</sub> curve with a ≥95% confidence interval. <sup>d</sup> Values are mean ± SEM for *n* = 3 (32) and 4 (33).

Having identified a racemic HDAC inhibitor **30** that demonstrates an improved balance of antitumor activity and hERG inhibition, we turned our attention to preparing its enantiomers. The *R* and *S* enantiomers of **30**, **32**, and **33** were prepared from chiral intermediates obtained by chromatographic resolution, using simulated moving bed (SMB) technology and a proprietary chiral stationary phase.<sup>21a,28</sup> Stereochemistry was determined by single-crystal X-ray analysis of one of the intermediates.<sup>21a,c</sup> The more potent HDAC inhibitor of the two enantiomers, **32**, turned out to also be less active in the hERG manual patch clamp assay (Table 4).<sup>21c,29</sup> Such separation of hERG activity between enantiomers has been observed previously.<sup>30</sup> It was also observed that **32** shows significantly improved cellular potency as measured by its inhibitory effect on cancer cell proliferation, even though its increased activity in the enzyme assay is less pronounced.<sup>31</sup> Compared to the parent compound dacinostat (**7**), **32** is 2-fold more potent at HDAC1 inhibition and 5-fold more potent against both HCT116 and H1299 cell lines. Isoform selectivity of **32** and **33** was also examined, proving both enantiomers to be pan-HDAC inhibitors with weaker activity against HDAC6 and HDAC8.<sup>21c</sup>

## Conclusion

In summary, rigidified analogues of dacinostat have been prepared to identify several novel scaffolds that display a combination of improved HDAC inhibition and reduced hERG inhibition. One such scaffold, based on 3-piperidin-3-ylindole, was investigated and led to the discovery of a potent HDAC inhibitor **30** with attenuated hERG inhibition. We proposed that this reduced inhibition is the result of the molecule's unique conformation, making interactions with the hERG channel less favorable. Separation of racemate **30** afforded the more potent HDAC inhibitor **32**, which exhibits reduced potency in the hERG manual patch clamp assay. Our approach of refining the three-dimensional structure of HDAC binding analogues was shown to benefit both HDAC and hERG potency profiles.

## Experimental Section

**HDAC Enzyme Assay.** The HDAC enzymatic assay measures compound activity in inhibiting purified HDAC isoforms. HDACs 1, 3, and 6 were immunopurified from 293 cells stably expressing the FLAG-tagged HDAC isoform, whereas HDACs 2, 4, 5, 7, 8, 9, 10, and 11 were purified from the baculovirus

expression system. HDAC activity was measured in a fluorescent assay in which deacetylation of the substrate, bis-Boc-(Ac)Lys-rhodamine 110, generates a fluorophore that can be detected on a fluorometric plate reader.

**Monolayer Cell Proliferation Assay.** Cells were plated at 5000–10000 cells per well in 96-well plates and treated with eight serial compound dilutions. Cell viability following 72 h of compound treatment was measured using the CellTiter-Glo or MTS assay. Assays were performed following the manufacture's protocol. XLfit 4 was used for plotting of the growth curves and calculation of IC<sub>50</sub> values.

**Chemistry.** All nonaqueous reactions were carried out under a nitrogen atmosphere unless otherwise noted. All solvents employed were commercially available “anhydrous” grade, and reagents were used as received unless otherwise noted. A Biotage Initiator Sixty system was used for microwave heating. Flash column chromatography was performed either on an Analogix Intelliflash 280 using Si 50 columns (32–63 μm, 230–400 mesh, 60 Å) or on a Biotage SP1 system (32–63 μm particle size, KP-Sil, 60 Å pore size). Preparative high pressure liquid chromatography (HPLC) was performed using a Waters 2525 pump with 2487 dual wavelength detector and 2767 sample manager. Columns were Waters C18 OBD 5 μm, either 50 mm × 100 mm Xbridge or 30 mm × 100 mm Sunfire. Systems were run with either a 5–95% or 10–90% ACN/H<sub>2</sub>O gradient with either a 0.1% TFA or 0.1% NH<sub>4</sub>OH modifier. NMR spectra were recorded on a Bruker AV400 (Avance 400 MHz) or AV500 (Avance 500 MHz) instruments. Analytical LC–MS was conducted using an Agilent 1100 series with UV detection at 214 and 254 nm and an electrospray mode (ESI) coupled with a Waters ZQ single quadrupole mass detector. One of two methods was used: (method A) 5–95% ACN/H<sub>2</sub>O with 5 mM ammonium formate with a 2 min run, 3 μL injection through an Inertsil C8 3 cm × 5 mm × 3 μm; (method B) 20–95% ACN/H<sub>2</sub>O with 10 mM ammonium formate with a 2 min run, 3 μL injection through an Inertsil C8 3 cm × 5 mm × 3 μm.

Analytical HPLC UV purity was assessed using an Agilent 1100 HPLC system and one of the following methods. For method 1 (at 214 nm), an Inertsil ODS3 3 μm, 3.0 mm × 100 mm C18 column was used with a flow rate of 1.5 mL/min and a gradient of 10–95% acetonitrile/water with 0.1% TFA over 15 min. For method 2 (at both 254 and 214 nm), an Inertsil ODS3 3 μm, 3.0 mm × 100 mm C18 column was used with a flow rate of 1.0 mL/min and a gradient of 5–95% acetonitrile/water with 0.1% TFA over 7.75 min. For method 3 (at both 254 and 215 nm), a Nova-Pak 4 μm, 3.9 mm × 150 mm C18 column was used with a flow rate of 2.0 mL/min and a gradient of 10–90% acetonitrile/water with 0.1% TFA over 5.0 min. LC/ESI-MS data were recorded using a Waters LCT Premier mass spectrometer with dual electrospray ionization source and Agilent 1100

liquid chromatograph. The resolution of the MS system was approximately 12 000 (fwhm definition). HPLC separation was performed at 1.0 mL/min flow rate with a gradient from 10% to 95% in 2.5 min. Ammonia formate (10 mM) was used as the modifier additive in the aqueous phase. Sulfadimethoxine (Sigma; protonated molecule  $m/z$  311.0814) was used as a reference and acquired through the LockSpray channel every third scan.

**General Procedure A for Preparation of 3-Piperidin-3-yl-1H-indoles.** **2-Methyl-3-piperidin-3-yl-1H-indole (19).** A mixture of 2-methyl-1H-indole (3.0 g, 22.6 mmol), 1-benzylpiperidin-3-one (11.3 g, 2.0 equiv), and 85%  $H_3PO_4$  in water (2.61 mL, 10 equiv) in glacial acetic acid (30 mL) was heated at 100 °C for 4 h. After cooling, the reaction mixture was diluted with EtOAc, washed with water and brine, dried over  $Na_2SO_4$ , filtered, and concentrated in vacuo to give a crude mixture of 3-(1-benzyl-1,2,5,6-tetrahydropyridin-3-yl)-2-methyl-1H-indole and 3-(1-benzyl-1,4,5,6-tetrahydropyridin-3-yl)-2-methyl-1H-indole (4.9 g, 72% yield). The crude mixture was diluted with MeOH (40 mL) and treated with  $Pd(OH)_2/C$  (20 wt %, wet, 2.0 g). The reaction bottle was evacuated and flushed with  $H_2$  three times and shaken under 50 psi in a Parr hydrogenator overnight. The reaction mixture was filtered through a pad of Celite and concentrated in vacuo to give the crude product 2-methyl-3-piperidin-3-yl-1H-indole (2.9 g, 83% yield).  $^1H$  NMR (400 MHz,  $CD_3OD$ )  $\delta$  7.46 (d,  $J$  = 7.7 Hz, 1 H), 7.23 (m, 1 H), 7.15 (m, 1 H), 7.04–6.94 (m, 1 H), 3.01 (m, 1 H), 2.75 (m, 2 H), 2.56 (m, 1 H), 2.30 (s, 3 H), 2.35 (m, 1 H), 1.83–1.21 (m, 6 H); MS  $m/z$  215.9 ( $M + H$ ) $^+$ .

**3-Piperidin-3-yl-1H-indole.** The compound was synthesized from 1H-indole following general procedure A in 54% yield over two steps.  $^1H$  NMR (400 MHz,  $CD_3OD$ )  $\delta$  7.58 (d,  $J$  = 8.0 Hz, 1 H), 7.32 (d,  $J$  = 8.0 Hz, 1 H), 7.07 (t,  $J$  = 8.0 Hz, 1 H), 7.00 (s, 1 H), 6.97 (d,  $J$  = 8.0 Hz, 1 H), 3.09–2.99 (m, 2 H), 2.63 (m, 2 H), 2.16 (d,  $J$  = 12 Hz, 1 H), 2.14 (m, 1 H), 1.80 (m, 1 H), 1.70 (m, 2 H).

**2-Phenyl-3-piperidin-3-yl-1H-indole.** The compound was synthesized from 2-phenyl-1H-indole following general procedure A in 96% yield over two steps.  $^1H$  NMR (400 MHz,  $DMSO-d_6$ )  $\delta$  11.2 (s, 1 H), 7.80 (d,  $J$  = 4.0 Hz, 1 H), 7.53 (m, 4 H), 7.42 (m, 1 H), 7.35 (d,  $J$  = 8.0 Hz, 1 H), 7.08 (t,  $J$  = 8.0 Hz, 1 H), 6.98 (t,  $J$  = 8.0 Hz, 1 H), 3.08 (m, 1 H), 2.99 (m, 2 H), 2.70 (m, 1 H), 2.15 (m, 1 H), 1.82 (m, 1 H), 1.70 (m, 1 H); MS  $m/z$  277.2 ( $M + H$ ) $^+$ .

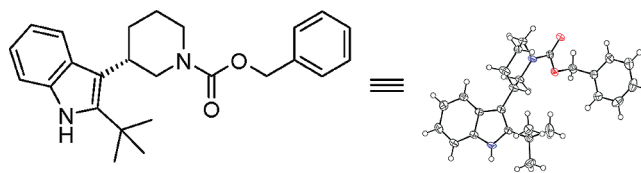
**2-tert-Butyl-3-piperidine-3-yl-1H-indole.** The compound was synthesized from 2-tert-butyl-1H-indole following general procedure A in 73% yield over two steps.  $^1H$  NMR (400 MHz,  $CDCl_3$ )  $\delta$  8.05 (br s, 1 H), 7.53 (d,  $J$  = 8.0 Hz, 1 H), 7.35 (d,  $J$  = 8.0 Hz, 1 H), 7.13 (t,  $J$  = 8.0 Hz, 1 H), 7.06 (t,  $J$  = 8.0 Hz, 1 H), 3.84 (m, 1 H), 3.58 (br d,  $J$  = 12 Hz, 1 H), 3.49 (m, 1 H), 3.41 (m, 1 H), 2.97 (m, 1 H), 2.96 (m, 2 H), 2.02 (br d,  $J$  = 12 Hz, 2 H), 1.51 (s, 9 H); MS  $m/z$  257.2 ( $M + H$ ) $^+$ .

**2-tert-Butyl-3-(S)-piperidin-3-yl-1H-indole and 2-tert-Butyl-3-(R)-piperidin-3-yl-1H-indole.** To a solution of 2-tert-butyl-3-piperidine-3-yl-1H-indole (5 g, 19.5 mmol) in  $CH_2Cl_2$  (200 mL) and *N*-methylmorpholine (10 mL) was added benzyl chloroformate (3.76 mL, 25.4 mmol, 1.3 equiv) dropwise over 10 min. The resulting mixture was stirred at 30 °C for 12 h. The reaction mixture was treated with saturated aqueous  $NaHCO_3$  (50 mL), and the phases were separated. The organic phase was dried over  $MgSO_4$ , filtered, and concentrated. Column chromatography (EtOAc/heptanes, 0–25%) afforded 3-(2-tert-butyl-1H-indol-3-yl)piperidine-1-carboxylic acid benzyl ester in 70% yield.  $^1H$  NMR (400 MHz,  $DMSO-d_6$ )  $\delta$  10.36 (br s, 1H), 7.65 (d,  $J$  = 8.0 Hz, 1 H), 7.45–7.25 (m, 6 H), 6.85–7.00 (m, 2 H), 4.95–5.15 (br m, 2 H), 3.90–4.15 (br m, 2 H), 3.35–3.65 (br m, 1 H), 3.15 (m, 2 H), 2.20 (m, 1 H), 1.77 (d,  $J$  = 12.0 Hz, 2 H), 1.45–1.55 (m, 1H), 1.44–1.25 (br m, 9H); MS  $m/z$  391.1 ( $M + H$ ) $^+$ .

An amount of 147 g of racemic 3-(2-tert-butyl-1H-indol-3-yl)piperidine-1-carboxylic acid benzyl ester was resolved by simulating moving bed (SMB) chromatography on a UOP-SORBEX

PREP instrument equipped with 16 columns (7.5 cm  $\times$  2.12 cm from Princeton Chromatography Corporation) containing the stationary phase FA-2392/6 (own phase, immobilized Amylose tris-(S)-methylbenzyl carbamate coated on 12  $\mu m$  silica gel): (mobile phase) hexane/2-propanol/EtOH, 75:15:10; (SMB parameters) feed concentration of 0.5% in the mobile phase (1.5 mL/min); (mobile phase) 12.7 mL/min; (extract rate) 3.0 mL/min; (cycle time) 60 min; (column configuration) 6–6–3–1. Chiral purity of the extract and raffinate was assessed by chiral HPLC using an Agilent 1200 HPLC system and a Chiralpak AS (Chiral Technologies, Illkirch, France) column (4.6 mm  $\times$  250 mm, 20  $\mu m$  material) at a flow rate of 1 mL/min, with a mixture of heptane/ethanol 95:5 (v/v) as the mobile phase  $t_{R1}$ (raffinate) = 13.76 min and  $t_{R2}$ (extract) = 23.61 min.

(1) The enantiomeric excess of enantiomer/raffinate was >99%. The X-ray crystal structure was determined for (S)-3-(2-tert-butyl-1H-indol-3-yl)piperidine-1-carboxylic acid benzyl ester.



(2) The enantiomeric excess of enantiomer/extract was 97%: (R)-3-(2-tert-butyl-1H-indol-3-yl)piperidine-1-carboxylic acid benzyl ester.

(S)-3-(2-tert-butyl-1H-indol-3-yl)piperidine-1-carboxylic acid benzyl ester (enantiomer/raffinate, 3 g, 7.68 mmol) was dissolved in MeOH (80 mL) and treated with HCl (32%, 10 M, 0.85 mL, 1.1 equiv) and Pd/C (10%, 600 mg). The mixture was degassed and subjected to hydrogenation in a Parr shaker for 2 h. The reaction mixture was filtered through a pad of Celite and concentrated. The crude product was partitioned between aqueous 1 M NaOH and  $CH_2Cl_2$ . The aqueous phase was reextracted with  $CH_2Cl_2$ . The organic phase was dried over  $MgSO_4$ , filtered, and concentrated to afford 2-tert-butyl-3-(S)-piperidin-3-yl-1H-indole in 83% yield.

**2-Methyl-3-pyrrolidin-3-yl-1H-indole (20).** A solution of malimide (5.63 g, 56.9 mmol) and 2-methyl-1H-indole (7.70 g, 1.02 equiv) in glacial acetic acid (50 mL) was heated to reflux for 3 days. After cooling, the reaction mixture was concentrated in vacuo to remove acetic acid and diluted with EtOAc (300 mL). The organic phase was washed with water (2  $\times$  100 mL), saturated aqueous  $NaHCO_3$  (3  $\times$  150 mL), dried over  $MgSO_4$ , filtered, and concentrated in vacuo. Column chromatography (EtOAc/hexanes, 20–60%) gave 3-(2-methyl-1H-indol-3-yl)pyrrolidine-2,5-dione (4.04 g) in 31% yield.  $^1H$  NMR (400 MHz,  $CDCl_3$ )  $\delta$  7.95 (br s, 1H), 7.30 (m, 2 H), 7.20–7.09 (m, 2 H), 4.32 (dd,  $J$  = 9.8, 5.7 Hz, 1H), 3.25 (dd,  $J$  = 19, 9.8 Hz, 1H), 3.05 (dd,  $J$  = 19, 5.7 Hz, 1H), 2.07 (s, 3 H).

To a solution of 3-(2-methyl-1H-indol-3-yl)pyrrolidine-2,5-dione (2.22 g, 9.73 mmol) and THF (100 mL) was added  $LiAlH_4$  (3.85 g, 10 equiv) portionwise, and the resulting mixture was heated to reflux for 20 h. The reaction mixture was cooled to 0 °C, treated carefully with EtOAc (7 mL) and water (3.5 mL), and stirred at room temperature for 20 min. The mixture was treated with 8.0 mL of 1 N aqueous solution of NaOH and 8.0 mL of water and then heated to reflux for 2 h. The mixture was cooled to room temperature and filtered. The filtrate was concentrated in vacuo. The remaining water was removed azeotropically with toluene to give the crude product 2-methyl-3-pyrrolidin-3-yl-1H-indole (1.95 g) in quantitative yield.  $^1H$  NMR (400 MHz,  $CD_3OD$ )  $\delta$  7.55 (m, 1 H), 7.25 (m, 1 H), 7.05–6.91 (m, 2 H), 3.65 (m, 1 H), 3.20–3.03 (m, 2 H), 2.70 (m, 2 H), 2.39 (s, 3 H), 2.24 (m, 2 H); MS  $m/z$  201.1 ( $M + H$ ) $^+$ .

**2-Methyl-3-piperidin-2-ylmethyl-1H-indole (21).** To a solution of *N*-Boc-2-piperidinecarboxylic acid (3.18 g, 13.6 mmol) in  $\text{CH}_2\text{Cl}_2$  (32 mL) with a trace of DMF (0.7 mL) was added oxalyl chloride (1.8 mL, 1.5 equiv), and the resulting mixture was stirred at room temperature for 1 h. The reaction mixture was concentrated in vacuo and further dried azeotropically with benzene. At the same time, a solution of  $\text{EtMgBr}$  in  $\text{Et}_2\text{O}$  (3.0 M, 9.0 mL, 2.1 equiv) was added dropwise to a cooled (0 °C) solution of 2-methyl-1H-indole (3.25 g, 1.8 equiv) in benzene (37 mL), and the resulting mixture was stirred at 0 °C for 9 min. Then the reaction mixture was treated with a solution of *N*-Boc-2-piperidinecarboxylic acid chloride in benzene (15 mL) dropwise with vigorous stirring. The resulting mixture was stirred at 0 °C for 1 h and treated with  $\text{EtOAc}$  (40 mL) and saturated aqueous  $\text{NaHCO}_3$  (35 mL), then stirred for 1 h. After separation, the aqueous phase was extracted with  $\text{EtOAc}$ . Combined organics were dried over  $\text{MgSO}_4$ , filtered, and concentrated in vacuo. Column chromatography ( $\text{MeOH}/\text{CH}_2\text{Cl}_2$ , 5–40%) gave (2-methyl-1H-indol-3-yl)piperidin-2-ylmethanone (0.550 g) in 17% yield.  $^1\text{H}$  NMR (400 MHz,  $\text{CD}_3\text{OD}$ )  $\delta$  7.86–7.84 (m, 1 H), 7.40–7.37 (m, 1 H), 7.21 (ddd,  $J = 13.0, 7.4, 1.5$  Hz, 1 H), 7.20 (ddd,  $J = 12.9, 7.5, 1.5$  Hz, 1 H), 4.26 (dd,  $J = 11.6, 2.7$  Hz, 1 H), 3.25–3.21 (m, 1 H), 2.83 (td,  $J = 12.8, 3.0$  Hz, 1 H), 2.74 (s, 3 H), 2.15–2.11 (m, 1 H), 2.00–1.95 (m, 1 H), 1.81–1.70 (m, 2 H), 1.58–1.47 (m, 1 H), 1.39 (ddd,  $J = 24.8, 12.3, 3.8$  Hz, 1 H); MS  $m/z$  243.1 ( $\text{M} + \text{H}$ ) $^+$ .

To a solution of (2-methyl-1H-indol-3-yl)piperidin-2-ylmethanone (491 mg, 2.03 mmol) in THF (20 mL) was added  $\text{LiAlH}_4$  (278 mg, 3.5 equiv), and the resulting mixture was stirred at room temperature for 2 h. The reaction mixture was quenched with 1 N NaOH (7.2 mL), stirred for 10 min, filtered, and concentrated in vacuo. The crude 2-methyl-3-piperidin-2-ylmethyl-1H-indole (0.47 g, quantitative yield) was used for the next reaction without purification.  $^1\text{H}$  NMR (400 MHz,  $\text{CD}_3\text{OD}$ )  $\delta$  7.46 (d,  $J = 7.7$  Hz, 1 H), 7.25–7.21 (m, 1 H), 7.18–7.11 (m, 1 H), 7.04–6.94 (m, 1 H), 3.03–2.99 (m, 1 H), 2.78–2.75 (m, 2 H), 2.60–2.53 (m, 1 H), 2.39 (s, 3 H), 2.35–2.34 (m, 1 H), 1.83–1.21 (m, 6 H); MS  $m/z$  229.1 ( $\text{M} + \text{H}$ ) $^+$ .

**General Procedure B for Preparation of Methyl Esters.** (*E*)-3-{4-[3-(2-Methyl-1H-indol-3-yl)piperidin-1-ylmethyl]phenyl}acrylic Acid Methyl Ester. 2-Methyl-3-piperidin-3-yl-1H-indole (19) (300 mg, 1.40 mmol) was diluted in  $\text{CH}_2\text{Cl}_2$  (20 mL) and treated with methyl 4-formylcinnamate (266 mg, 1 equiv) and triethylamine (0.58 mL, 3.0 equiv). The resulting mixture was treated with  $\text{TiCl}_4$  (0.67 mL, 0.48 equiv) dropwise. Once 2-methyl-3-piperidin-3-yl-1H-indole was consumed, the reaction mixture was treated with  $\text{NaBH}_3\text{CN}$  (278 mg, 3.0 equiv). After 2 h, the reaction mixture was basified to pH 13 with 5 N NaOH and extracted with  $\text{EtOAc}$ . Combined organic phase was dried over  $\text{Na}_2\text{SO}_4$ , filtered, and concentrated in vacuo. Column chromatography afforded (*E*)-3-{4-[3-(2-methyl-1H-indol-3-yl)piperidin-1-ylmethyl]phenyl}acrylic acid methyl ester (140 mg) in 26% yield.  $^1\text{H}$  NMR (400 MHz,  $\text{CDCl}_3$ )  $\delta$  7.75 (br s, 1 H), 7.70 (m, 2 H), 7.48 (d,  $J = 8.0$  Hz, 2 H), 7.38 (d,  $J = 8.0$  Hz, 2 H), 7.27 (d,  $J = 8.0$  Hz, 1 H), 7.12–7.04 (m, 2 H), 6.44 (d,  $J = 16$  Hz, 1 H), 3.82 (s, 3 H), 3.58 (s, 2 H), 3.11 (m, 1 H), 2.96 (m, 2 H), 2.54 (t,  $J = 8.0$  Hz, 1 H), 2.53 (m, 1 H), 2.41 (s, 3 H), 2.09 (m, 1 H), 1.92 (m, 1 H), 1.64 (m, 2 H); MS  $m/z$  389.0 ( $\text{M} + \text{H}$ ) $^+$ .

(*E*)-3-{4-[3-(1H-Indol-3-yl)piperidin-1-ylmethyl]phenyl}acrylic Acid Methyl Ester. The compound was synthesized from 3-piperidin-3-yl-1H-indole following general procedure B in 45% yield.  $^1\text{H}$  NMR (400 MHz,  $\text{CDCl}_3$ )  $\delta$  7.97 (br s, 1 H), 7.70 (d,  $J = 16$  Hz, 1 H), 7.64 (d,  $J = 8.0$  Hz, 1 H), 7.48 (d,  $J = 8.0$  Hz, 2 H), 7.38 (d,  $J = 8.0$  Hz, 2 H), 7.36 (d,  $J = 8.0$  Hz, 1 H), 7.18 (m, 1 H), 7.10 (m, 1 H), 7.01 (br d,  $J = 2.0$  Hz, 1 H), 6.43 (d,  $J = 16$  Hz, 1 H), 3.82 (s, 3 H), 3.58 (br s, 2 H), 3.19 (m, 2 H), 2.91 (m, 1 H), 2.11 (m, 2 H), 1.79 (m, 2 H), 1.56 (m, 2 H); MS  $m/z$  374.9 ( $\text{M} + \text{H}$ ) $^+$ .

(*E*)-3-{4-[2-(2-Methyl-1H-indol-3-ylmethyl)piperidin-1-ylmethyl]phenyl}acrylic Acid Methyl Ester. The compound was synthesized from 2-methyl-3-piperidin-2-ylmethyl-1H-indole following general procedure B in 47% yield. MS  $m/z$  403.9 ( $\text{M} + \text{H}$ ) $^+$ .

**General Procedure C for Preparation of Methyl Esters.** (*E*)-3-{4-[3-(2-Phenyl-1H-indol-3-yl)piperidin-1-ylmethyl]phenyl}acrylic Acid Methyl Ester. 2-Phenyl-3-piperidin-3-yl-1H-indole (2.0 g, 7.16 mmol) was dissolved in  $\text{CH}_2\text{Cl}_2$  (20 mL) and treated with triethylamine (3.0 mL, 3.0 equiv) and 4-bromobenzyl bromide (1.97 g, 1.1 equiv). After being stirred for 4 h, the reaction mixture was diluted with  $\text{EtOAc}$ , washed with water and brine, dried over  $\text{MgSO}_4$ , filtered, and concentrated in vacuo. Column chromatography ( $\text{EtOAc}/\text{hexanes}$ , 0–90%) provided 3-[1-(4-bromobenzyl)piperidin-3-yl]-2-phenyl-1H-indole (2.1 g) in 66% yield.  $^1\text{H}$  NMR (400 MHz,  $\text{CDCl}_3$ )  $\delta$  8.00 (br s, 1 H), 7.86 (d,  $J = 8.0$  Hz, 1 H), 7.51–7.40 (m, 7 H), 7.37 (d,  $J = 8.0$  Hz, 1 H), 7.23–7.11 (m, 4 H), 3.51 (dd,  $J = 20, 12$  Hz, 2 H), 3.31 (m, 1 H), 2.96 (m, 2 H), 2.08 (m, 2 H), 1.92 (m, 1 H), 1.81–1.66 (m, 2 H); MS  $m/z$  447.1 ( $\text{M} + \text{H}$ ) $^+$ .

A microwave vial was charged with a solution of 3-[1-(4-bromobenzyl)piperidin-3-yl]-2-phenyl-1H-indole (500 mg, 1.11 mmol) in 1,4-dioxane (10 mL) and tri-*tert*-butylphosphonium tetrafluoroborate (13 mg, 0.04 equiv) and  $\text{Pd}_2(\text{dba})_3$  (10 mg, 0.01 equiv), then flushed with nitrogen three times. The resulting mixture was treated with  $\text{Cy}_2\text{NMe}$  (0.28 mL, 1.2 equiv) and methyl acrylate (0.20 mL, 2.0 equiv), then heated at 100 °C by microwave for 1 h. The reaction mixture was diluted with  $\text{EtOAc}$ , washed with water and brine, dried over  $\text{MgSO}_4$ , filtered, and concentrated in vacuo. Column chromatography ( $\text{MeOH}/\text{CH}_2\text{Cl}_2$ , 0–15%) gave (*E*)-3-{4-[3-(2-phenyl-1H-indol-3-yl)piperidin-1-ylmethyl]phenyl}acrylic acid methyl ester (310 mg) in 62% yield.  $^1\text{H}$  NMR (400 MHz,  $\text{CDCl}_3$ )  $\delta$  8.01 (br s, 1 H), 7.86 (d,  $J = 8.0$  Hz, 1 H), 7.69 (d,  $J = 16$  Hz, 1 H), 7.50–7.34 (m, 10 H), 7.20–7.10 (m, 2 H), 6.42 (d,  $J = 16$  Hz, 1 H), 3.81 (s, 3 H), 3.57 (dd,  $J = 20, 12$  Hz, 2 H), 3.31 (m, 1 H), 2.97 (m, 2 H), 2.68 (t,  $J = 10$  Hz, 1 H), 2.15–2.04 (m, 2 H), 1.92 (br d,  $J = 8.0$  Hz, 1 H), 1.76 (m, 2 H); MS  $m/z$  451.0 ( $\text{M} + \text{H}$ ) $^+$ .

(*E*)-3-{4-[3-(2-*tert*-Butyl-1H-indol-3-yl)piperidin-1-ylmethyl]phenyl}acrylic Acid Methyl Ester. The compound was synthesized from 2-*tert*-butyl-3-piperidine-3-yl-1H-indole following general procedure C in 66% yield over two steps.

3-[1-(4-Bromobenzyl)piperidin-3-yl]-2-*tert*-butyl-1H-indole:  $^1\text{H}$  NMR (400 MHz,  $\text{CDCl}_3$ )  $\delta$  7.87 (br s, 1 H), 7.75 (d,  $J = 8.0$  Hz, 1 H), 7.41 (d,  $J = 8.0$  Hz, 2 H), 7.31 (d,  $J = 8.0$  Hz, 1 H), 7.24 (d,  $J = 8.0$  Hz, 2 H), 7.12–7.03 (m, 2 H), 3.53 (dd,  $J = 44, 12$  Hz, 2 H), 3.40 (tt,  $J = 12, 3.7$  Hz, 1 H), 2.99 (br d,  $J = 11$  Hz, 1 H), 2.88 (br d,  $J = 11$  Hz, 1 H), 2.63 (t,  $J = 12$  Hz, 1 H), 2.20–2.05 (m, 2 H), 1.83 (m, 3 H), 1.47 (s, 9 H); MS  $m/z$  426.8 ( $\text{M} + \text{H}$ ) $^+$ .

(*E*)-3-{4-[3-(2-*tert*-Butyl-1H-indol-3-yl)piperidin-1-ylmethyl]phenyl}acrylic acid methyl ester:  $^1\text{H}$  NMR (400 MHz,  $\text{CDCl}_3$ )  $\delta$  7.88 (br s, 1 H), 7.75 (d,  $J = 8.0$  Hz, 1 H), 7.69 (d,  $J = 16$  Hz, 1 H), 7.46 (d,  $J = 8.0$  Hz, 2 H), 7.39 (d,  $J = 8.0$  Hz, 2 H), 7.30 (d,  $J = 8.0$  Hz, 1 H), 7.11–7.02 (m, 2 H), 6.43 (d,  $J = 16$  Hz, 1 H), 3.82 (s, 3 H), 3.60 (dd,  $J = 50, 14$  Hz, 2 H), 3.42 (m, 1 H), 3.02 (br d,  $J = 12$  Hz, 1 H), 2.89 (br d,  $J = 12$  Hz, 1 H), 2.64 (t,  $J = 10$  Hz, 1 H), 2.16 (m, 2 H), 1.84 (m, 3 H), 1.46 (s, 9 H); MS  $m/z$  430.9 ( $\text{M} + \text{H}$ ) $^+$ .

(*E*)-3-{4-[2-(2-Methyl-1H-indol-3-yl)pyrrolidin-1-ylmethyl]phenyl}acrylic Acid Methyl Ester. The compound was synthesized from 2-methyl-3-pyrrolidin-3-yl-1H-indole following general procedure C in 12% yield over two steps.

3-[1-(4-Bromobenzyl)pyrrolidin-2-yl]-2-methyl-1H-indole:  $^1\text{H}$  NMR (400 MHz,  $\text{CDCl}_3$ )  $\delta$  8.15 (s, 1 H), 7.98 (m, 1 H), 7.58 (d,  $J = 7.8$  Hz, 2 H), 7.39 (d,  $J = 8.4$  Hz, 2 H), 7.31 (m, 3 H), 3.81 (s, 2 H), 3.76 (m, 1 H), 3.10–2.91 (m, 4 H), 2.43–2.39 (m, 2 H), 2.38 (s, 3 H); MS  $m/z$  371.0 ( $\text{M} + \text{H}$ ) $^+$ .

(*E*)-3-{4-[2-(2-Methyl-1H-indol-3-yl)pyrrolidin-1-ylmethyl]phenyl}acrylic Acid Methyl Ester:  $^1\text{H}$  NMR (400 MHz,  $\text{CD}_3\text{OD}$ )  $\delta$  7.58 (m, 2 H), 7.34 (d,  $J = 7.6$  Hz, 2 H), 7.22 (m, 3 H), 6.99 (m, 2 H), 6.39 (d,  $J = 16.1$  Hz, 1 H), 3.72 (s, 3 H), 3.54 (m, 1 H), 3.50 (s, 2 H), 2.83–2.73 (m, 2 H), 2.68–2.58 (m, 2 H), 2.27 (s, 3 H), 2.13–2.06 (m, 2 H); MS  $m/z$  375.1 ( $\text{M} + \text{H}$ ) $^+$ .

(*E*)-3-{3-Fluoro-4-[3-(1H-indol-3-yl)piperidin-1-ylmethyl]phenyl}acrylic Acid Methyl Ester. The compound was synthesized from 3-piperidin-3-yl-1H-indole and 4-bromo-2-fluorobenzyl

bromide following general procedure C in 10% yield over two steps.

**3-[1-(4-Bromobenzyl)piperidin-3-yl]-1H-indole:**  $^1\text{H}$  NMR (400 MHz,  $\text{CDCl}_3$ )  $\delta$  8.04 (br s, 1 H), 7.66 (d,  $J$  = 8.0 Hz, 1 H), 7.38–7.11 (m, 6 H), 7.02 (d,  $J$  = 4.0 Hz, 1 H), 3.63 (br d,  $J$  = 4.0 Hz, 2 H), 3.21 (m, 2 H), 2.93 (m, 1 H), 2.69 (t,  $J$  = 8.0 Hz, 1 H), 2.38 (t,  $J$  = 8.0 Hz, 1 H), 2.12 (m, 1 H), 1.98 (m, 1 H), 1.80 (m, 2 H), 1.53 (m, 1 H); MS  $m/z$  388.8 ( $\text{M} + \text{H}$ ) $^+$ .

**(E)-3-{3-Fluoro-4-[3-(1H-indol-3-yl)piperidin-1-ylmethyl]phenyl}acrylic acid methyl ester:**  $^1\text{H}$  NMR (400 MHz,  $\text{CDCl}_3$ )  $\delta$  8.10 (br s, 1 H), 7.65 (m, 2 H), 7.48 (t,  $J$  = 8.0 Hz, 1 H), 7.37 (d,  $J$  = 8.0 Hz, 1 H), 7.29 (m, 1 H), 7.19 (m, 2 H), 7.11 (m, 1 H), 7.03 (m, 1 H), 6.43 (d,  $J$  = 16 Hz, 1 H), 3.83 (s, 3 H), 3.66 (br s, 2 H), 3.22 (m, 2 H), 2.94 (m, 1 H), 2.54 (m, 1 H), 2.34–2.07 (m, 3 H), 1.65–1.50 (m, 2 H).

**(E)-3-{3-Fluoro-4-[3-(2-phenyl-1H-indol-3-yl)piperidin-1-ylmethyl]phenyl}acrylic Acid Methyl Ester.** The compound was synthesized from 2-phenyl-3-piperidin-3-yl-1H-indole and 4-bromo-2-fluorobenzyl bromide following general procedure C in 26% yield over two steps.

**3-[1-(2-Fluoro-4-methylbenzyl)piperidin-3-yl]-2-phenyl-1H-indole:**  $^1\text{H}$  NMR (400 MHz,  $\text{CDCl}_3$ )  $\delta$  7.99 (br s, 1 H), 7.85 (d,  $J$  = 8.0 Hz, 1 H), 7.51–7.38 (m, 6 H), 7.33–7.11 (m, 5 H), 3.59 (br s, 2 H), 3.31 (m, 1 H), 2.97 (m, 2 H), 2.74 (t,  $J$  = 10 Hz, 1 H), 2.17 (m, 1 H), 2.95 (m, 1 H), 1.93 (m, 1 H), 1.78 (m, 2 H); MS  $m/z$  462.7 ( $\text{M} + \text{H}$ ) $^+$ .

**(E)-3-{3-Fluoro-4-[3-(2-phenyl-1H-indol-3-yl)piperidin-1-ylmethyl]phenyl}acrylic acid methyl ester:**  $^1\text{H}$  NMR (400 MHz,  $\text{CDCl}_3$ )  $\delta$  8.00 (br s, 1 H), 7.84 (d,  $J$  = 8.0 Hz, 1 H), 7.63 (d,  $J$  = 16 Hz, 1 H), 7.48–7.36 (m, 7 H), 7.26–7.09 (m, 4 H), 6.41 (d,  $J$  = 16 Hz, 1 H), 3.81 (s, 3 H), 3.64 (s, 2 H), 3.31 (m, 1 H), 2.99 (m, 2 H), 2.74 (t,  $J$  = 12 Hz, 1 H), 2.18 (m, 1 H), 2.05 (m, 1 H), 1.91 (m, 1 H), 1.71 (m, 1 H), 1.62 (m, 1 H); MS  $m/z$  468.8 ( $\text{M} + \text{H}$ ) $^+$ .

**(E)-3-{4-[3-(2-tert-Butyl-1H-indol-3-yl)piperidin-1-ylmethyl]-3-fluorophenyl}acrylic Acid Methyl Ester.** The compound was synthesized from 2-tert-butyl-3-piperidine-3-yl-1H-indole and 4-bromo-2-fluorobenzyl bromide following general procedure C in 67% yield over two steps.

**3-[1-(4-Bromo-2-fluorobenzyl)piperidin-3-yl]-2-tert-butyl-1H-indole:**  $^1\text{H}$  NMR (400 MHz,  $\text{CDCl}_3$ )  $\delta$  7.88 (br s, 1 H), 7.74 (d,  $J$  = 8.0 Hz, 1 H), 7.36 (t,  $J$  = 8.0 Hz, 1 H), 7.31 (d,  $J$  = 8.0 Hz, 1 H), 7.23 (d,  $J$  = 8.0 Hz, 1 H), 7.20 (d,  $J$  = 8.0 Hz, 1 H), 7.10 (t,  $J$  = 8.0 Hz, 1 H), 7.05 (t,  $J$  = 8.0 Hz, 1 H), 3.61 (br s, 2 H), 3.41 (m, 1 H), 3.01 (br d,  $J$  = 12 Hz, 1 H), 2.90 (br d,  $J$  = 12 Hz, 1 H), 2.72 (t,  $J$  = 10 Hz, 1 H), 2.25–2.04 (m, 2 H), 1.84 (m, 3 H), 1.47 (s, 9 H).

**(E)-3-{4-[3-(2-tert-Butyl-1H-indol-3-yl)piperidin-1-ylmethyl]-3-fluorophenyl}acrylic acid methyl ester:**  $^1\text{H}$  NMR (400 MHz,  $\text{CDCl}_3$ )  $\delta$  7.88 (br s, 1 H), 7.74, (d,  $J$  = 4.0 Hz, 1 H), 7.64 (d,  $J$  = 16 Hz, 1 H), 7.50 (t,  $J$  = 8.0 Hz, 1 H), 7.31 (d,  $J$  = 8.0 Hz, 1 H), 7.25 (d,  $J$  = 8.0 Hz, 1 H), 7.18 (d,  $J$  = 12 Hz, 1 H), 7.10 (t,  $J$  = 8.0 Hz, 1 H), 7.04 (t,  $J$  = 8.0 Hz, 1 H), 6.42 (d,  $J$  = 16 Hz, 1 H), 3.83 (s, 3 H), 3.66 (br s, 2 H), 3.42 (m, 1 H), 3.03 (br d,  $J$  = 12 Hz, 1 H), 2.92 (br d,  $J$  = 12 Hz, 1 H), 2.73 (t,  $J$  = 12 Hz, 1 H), 2.24 (m, 1 H), 2.09 (m, 1 H), 1.85 (m, 3 H), 1.47 (s, 9 H); MS  $m/z$  449.1 ( $\text{M} + \text{H}$ ) $^+$ .

**(E)-3-{4-[3-(2-tert-Butyl-1H-indol-3-yl)piperidin-1-ylmethyl]-3-chlorophenyl}acrylic Acid Methyl Ester.** To a solution of 4-bromo-2-chlorobenzoic acid (300 mg, 1.26 mmol) in DMF (3 mL) were added HBTU (717 mg, 1.5 equiv), HOBt (255 mg, 1.5 equiv), and DIPEA (0.88 mL, 4.0 equiv), and the resulting mixture was stirred at room temperature for 20 min. The reaction mixture was treated with 2-tert-butyl-3-piperidine-3-yl-1H-indole (400 mg, 1.2 equiv) and stirred for additional 4 h. The reaction mixture was quenched with water, diluted with EtOAc, washed with water and brine, dried over  $\text{Na}_2\text{SO}_4$ , filtered, and concentrated in vacuo. The crude product (4-bromo-2-chlorophenyl)-[3-(2-tert-butyl-1H-indol-3-yl)piperidin-1-yl]-methanone was dissolved in THF (10 mL) and treated with a solution of borane tetrahydrofuran complex in THF (1.0 M,

3.3 mL). The resulting mixture was stirred at room temperature for 4 h. To the reaction mixture was added MeOH (5 mL) dropwise followed by addition of 1 N aqueous solution of HCl (10 mL). The resulting mixture was heated to reflux for 3 h. After cooling, the reaction mixture was diluted with EtOAc, washed with water and brine, dried over  $\text{Na}_2\text{SO}_4$ , filtered, and concentrated in vacuo. Column chromatography (EtOAc/hexanes, 10–100%) gave 3-[1-(4-bromo-2-chlorobenzyl)piperidin-3-yl]-2-tert-butyl-1H-indole (270 mg) in 47% yield over two steps.  $^1\text{H}$  NMR (400 MHz,  $\text{CDCl}_3$ )  $\delta$  8.02 (br s, 1 H), 7.94 (d,  $J$  = 8.0 Hz, 1 H), 7.64–7.60 (m, 2 H), 7.47 (dd,  $J$  = 8.0 Hz, 1 H), 7.43 (d,  $J$  = 8.0 Hz, 1 H), 7.24 (qd,  $J$  = 8.0, 2.0 Hz, 1 H), 3.76 (s, 2 H), 3.59 (tt,  $J$  = 12, 4.0 Hz, 1 H), 3.14 (br d,  $J$  = 12 Hz, 1 H), 3.07 (m, 1 H), 2.92 (t,  $J$  = 12 Hz, 1 H), 2.42 (td,  $J$  = 10, 2.0 Hz, 1 H), 2.27 (m, 1 H), 2.05–1.92 (m, 3 H), 1.61 (s, 9 H); MS  $m/z$  459.0 ( $\text{M} + \text{H}$ ) $^+$ .

Following the second part of general procedure C, (E)-3-{4-[3-(2-tert-butyl-1H-indol-3-yl)piperidin-1-ylmethyl]-3-chlorophenyl}acrylic acid methyl ester was prepared.  $^1\text{H}$  NMR (400 MHz,  $\text{CDCl}_3$ )  $\delta$  7.81 (br s, 1 H), 7.68 (d,  $J$  = 8.0 Hz, 1 H), 7.53 (d,  $J$  = 8.0 Hz, 1 H), 7.52 (d,  $J$  = 16 Hz, 1 H), 7.39 (d,  $J$  = 1.6 Hz, 1 H), 7.2 (dd,  $J$  = 8.0, 1.5 Hz, 1 H), 7.19 (d,  $J$  = 8.0 Hz, 1 H), 7.00 (m, 1 H), 6.95 (m, 1 H), 6.32 (d,  $J$  = 16 Hz, 1 H), 3.73 (s, 3 H), 3.58 (s, 2 H), 3.34 (m, 1 H), 2.92 (br d,  $J$  = 11 Hz, 1 H), 2.82 (br dd,  $J$  = 11, 3.7 Hz, 1 H), 2.68 (t,  $J$  = 11 Hz, 1 H), 2.19 (m, 1 H), 2.02 (m, 1 H), 1.76 (m, 3 H), 1.38 (s, 9 H); MS  $m/z$  465.1 ( $\text{M} + \text{H}$ ) $^+$ .

**(E)-3-(4-{1-[2-(2-Methyl-1H-indol-3-yl)ethyl]pyrrolidin-2-yl}-phenyl)acrylic Acid Methyl Ester (14).** (2-Methyl-1H-indol-3-yl)-acetaldehyde (**23**, 495 mg, 1.5 equiv) was diluted in  $\text{CH}_2\text{Cl}_2$  (20 mL) and treated with 2-(4-bromophenyl)pyrrolidine (**24**, 430 mg, 1.904 mmol) and triethylamine (0.42 mL, 3.0 equiv). The resulting mixture was treated with  $\text{TiCl}_4$  (0.72 mL, 0.50 equiv) dropwise. Once 2-(4-bromophenyl)pyrrolidine was consumed, the reaction mixture was treated with  $\text{NaBH}_3\text{CN}$  (286 mg, 3.0 equiv). After 2 h, the reaction mixture was basified to pH 13 with 5 N NaOH and extracted with EtOAc. Combined organic phase was dried over  $\text{Na}_2\text{SO}_4$ , filtered, and concentrated in vacuo. Column chromatography (EtOAc/heptanes, 0–40%) afforded 3-{2-[2-(4-bromophenyl)pyrrolidin-1-yl]ethyl}-2-methyl-1H-indole (365 mg) in 50% yield.  $^1\text{H}$  NMR (400 MHz,  $\text{CDCl}_3$ )  $\delta$  7.70 (br s, 1 H), 7.40 (d,  $J$  = 8.0 Hz, 1 H), 7.34 (d,  $J$  = 8.0 Hz, 1 H), 7.25 (d,  $J$  = 8.0 Hz, 1 H), 7.21 (d,  $J$  = 8.0 Hz, 1 H), 7.11–7.01 (m, 2 H), 3.55 (m, 1 H), 3.27 (m, 1 H), 2.92–2.70 (m, 3 H), 2.42 (m, 1 H), 2.33 (m, 2 H), 2.30 (s, 3 H), 2.17 (m, 1 H), 2.00 (m, 1 H), 1.88 (m, 1 H); MS  $m/z$  384.8 ( $\text{M} + \text{H}$ ) $^+$ .

A microwave vial was charged with a solution of 3-{2-[2-(4-bromophenyl)pyrrolidin-1-yl]ethyl}-2-methyl-1H-indole (290 mg, 0.757 mmol) in 1,4-dioxane (10 mL), tri-tert-butylphosphonium tetrafluoroborate (8.8 mg, 0.04 equiv), and  $\text{Pd}_2(\text{dba})_3$  (6.9 mg, 0.01 equiv), then flushed with nitrogen three times. The resulting mixture was treated with  $\text{C}_2\text{NMe}$  (0.19 mL, 1.2 equiv) and methyl acrylate (0.14 mL, 2.0 equiv), then heated at 100 °C by microwave for 1 h. The reaction mixture was diluted with EtOAc, washed with water and brine, dried over  $\text{MgSO}_4$ , filtered, and concentrated in vacuo. Column chromatography (EtOAc/heptanes, 0–50%) gave (E)-3-(4-{1-[2-(2-methyl-1H-indol-3-yl)-ethyl]pyrrolidin-2-yl}phenyl)acrylic acid methyl ester (285 mg) in 97% yield.  $^1\text{H}$  NMR (400 MHz,  $\text{CDCl}_3$ )  $\delta$  7.92 (d,  $J$  = 16 Hz, 1 H), 7.92 (br s, 1 H), 7.66 (m, 2 H), 7.56 (m, 3 H), 7.47 (d,  $J$  = 8.0 Hz, 1 H), 7.33–7.21 (m, 2 H), 6.65 (d,  $J$  = 16 Hz, 1 H), 4.05 (s, 3 H), 3.79 (m, 1 H), 3.55 (m, 1 H), 3.10 (m, 1 H), 2.99 (m, 2 H), 2.65 (m, 1 H), 2.57 (m, 1 H), 2.52 (s, 3 H), 2.42 (m, 1 H), 2.23 (m, 1 H), 2.12 (m, 1 H), 1.94 (m, 1 H); MS  $m/z$  389.3 ( $\text{M} + \text{H}$ ) $^+$ .

**General Procedure D for Preparation of Hydroxamic Acids.** (E)-N-Hydroxy-3-[4-[3-(2-methyl-1H-indol-3-yl)piperidin-1-ylmethyl]phenyl]acrylamide (**11**). To a cooled (0 °C) solution of (E)-3-[4-[3-(2-methyl-1H-indol-3-yl)piperidin-1-ylmethyl]phenyl]acrylic acid methyl ester (640 mg, 1.63 mmol) in MeOH (3 mL) was added a solution of  $\text{NH}_2\text{OH}$  in water (50%, 1.08 mL, 10 equiv) followed by a solution of NaOMe in MeOH (25%, 1.76 mL, 5 equiv), and

the resulting mixture was stirred at 0 °C for 2  $\frac{1}{2}$  h. The reaction mixture was neutralized with a 1 N aqueous solution of HCl until the pH was 7–8. Precipitate was collected, washed with Et<sub>2</sub>O, and dried to provide (*E*)-*N*-hydroxy-3-{4-[3-(2-methyl-1*H*-indol-3-yl)piperidin-1-ylmethyl]phenyl}acrylamide (461 mg) in 73% yield. <sup>1</sup>H NMR (400 MHz, CD<sub>3</sub>OD)  $\delta$  7.57–7.47 (m, 4 H), 7.33 (d, *J* = 8.0 Hz, 2 H), 7.22 (d, *J* = 8.0 Hz, 1 H), 6.98 (t, *J* = 8.0 Hz, 1 H), 6.92 (t, *J* = 8.0 Hz, 1 H), 6.45 (d, *J* = 16 Hz, 1 H), 3.55 (dd, *J* = 20, 12 Hz, 2 H), 3.11 (m, 1 H), 2.99 (br d, *J* = 12 Hz, 1 H), 2.86 (br d, *J* = 12 Hz, 1 H), 2.53 (t, *J* = 12 Hz, 1 H), 2.35 (s, 3 H), 2.12 (m, 1 H), 1.95 (m, 1 H), 1.80 (m, 3 H). Anal. RP-HPLC *t*<sub>R</sub> = 2.62 min (method 3, purity 100.00%/100.00%). HR-MS *m/z* (M + H)<sup>+</sup>: measd 390.2175, calcd 390.2182.

(*E*)-*N*-Hydroxy-3-{4-[3-(2-methyl-1*H*-indol-3-yl)pyrrolidin-1-ylmethyl]phenyl}acrylamide (12). 12 was synthesized from (*E*)-3-{4-[2-(2-methyl-1*H*-indol-3-yl)pyrrolidin-1-ylmethyl]phenyl}-acrylic acid methyl ester following general procedure D in 87% yield. <sup>1</sup>H NMR (400 MHz, CD<sub>3</sub>OD)  $\delta$  7.60 (d, *J* = 8.0 Hz, 2 H), 7.56 (d, *J* = 8.0 Hz, 2 H), 7.47 (d, *J* = 8.0 Hz, 2 H), 7.24 (d, *J* = 8.0 Hz, 1 H), 7.01 (m, 1 H), 6.94 (m, 1 H), 6.48 (d, *J* = 16 Hz, 1 H), 3.84 (dd, *J* = 20, 12 Hz, 2 H), 3.67 (q, *J* = 8.0 Hz, 1 H), 3.08–2.80 (m, 4 H), 2.37 (s, 3 H), 2.24 (q, *J* = 8.0 Hz, 2 H). Anal. RP-HPLC *t*<sub>R</sub> = 3.23 min (method 1, purity 100.00%). HR-MS *m/z* (M + H)<sup>+</sup>: measd 376.2014, calcd 376.2025.

(*E*)-*N*-Hydroxy-3-{4-[2-(2-methyl-1*H*-indol-3-ylmethyl)piperidin-1-ylmethyl]phenyl}acrylamide (13). 13 was synthesized from (*E*)-3-{4-[2-(2-methyl-1*H*-indol-3-ylmethyl)piperidin-1-ylmethyl]phenyl}-acrylic acid methyl ester following general procedure D in 17% yield. <sup>1</sup>H NMR (400 MHz, CD<sub>3</sub>OD)  $\delta$  7.60–7.42 (m, 5 H), 7.25 (d, *J* = 8.0 Hz, 2 H), 7.20 (d, *J* = 8.0 Hz, 2 H), 6.96 (t, *J* = 8.0 Hz, 1 H), 6.87 (t, *J* = 8.0 Hz, 1 H), 6.49 (d, *J* = 16 Hz, 1 H), 4.29 (d, *J* = 12 Hz, 1 H), 3.59 (d, *J* = 12 Hz, 1 H), 2.89 (m, 2 H), 2.72 (m, 3 H), 2.35 (s, 3 H), 1.68 (m, 1 H), 1.54 (m, 2 H), 1.28 (m, 2 H). Anal. RP-HPLC *t*<sub>R</sub> = 3.45 min (method 1, purity 100.00%). HR-MS *m/z* (M + H)<sup>+</sup>: measd 404.2338, calcd 404.2338.

(*E*)-*N*-Hydroxy-3-{4-[1-[2-(2-methyl-1*H*-indol-3-yl)ethyl]pyrrolidin-2-yl]phenyl}acrylamide (14). 14 was synthesized from (*E*)-3-{4-[1-[2-(2-methyl-1*H*-indol-3-yl)ethyl]pyrrolidin-2-yl]phenyl}-acrylic acid methyl ester following general procedure D in 65% yield. <sup>1</sup>H NMR (400 MHz, CD<sub>3</sub>OD)  $\delta$  7.54 (d, *J* = 16 Hz, 1 H), 7.44 (d, *J* = 8.0 Hz, 2 H), 7.31 (d, *J* = 8.0 Hz, 2 H), 7.18 (d, *J* = 8.0 Hz, 2 H), 6.93 (m, 1 H), 6.83 (m, 1 H), 6.44 (d, *J* = 16 Hz, 1 H), 3.51 (m, 1 H), 2.83 (m, 1 H), 2.72 (m, 2 H), 2.43 (m, 2 H), 2.30–2.15 (m, 2 H), 2.23 (s, 3 H), 1.93 (m, 2 H), 1.71 (m, 1 H). Anal. RP-HPLC *t*<sub>R</sub> = 3.16 min (method 1, purity 93.70%). HR-MS *m/z* (M + H)<sup>+</sup>: measd 390.2174, calcd 390.2182.

(*E*)-*N*-Hydroxy-3-{4-[3-(1*H*-indol-3-yl)piperidin-1-ylmethyl]phenyl}acrylamide (25). 25 was synthesized from (*E*)-3-{4-[3-(1*H*-indol-3-yl)piperidin-1-ylmethyl]phenyl}-acrylic acid methyl ester following general procedure D in 38% yield. <sup>1</sup>H NMR (400 MHz, CD<sub>3</sub>OD)  $\delta$  7.38 (m, 4 H), 7.22 (m, 3 H), 6.95 (m, 1 H), 6.89 (s, 1 H), 6.85 (m, 1 H), 6.39 (d, *J* = 16 Hz, 1 H), 3.43 (s, 2 H), 3.05 (m, 2 H), 2.83 (m, 1 H), 1.95 (m, 3 H), 1.68 (m, 2 H), 1.43 (m, 1 H). Anal. RP-HPLC *t*<sub>R</sub> = 2.74 min (method 2, purity 100.00%/100.00%). HR-MS *m/z* (M + H)<sup>+</sup>: measd 376.2029, calcd 376.2025.

(*E*)-*N*-Hydroxy-3-{4-[3-(2-phenyl-1*H*-indol-3-yl)piperidin-1-ylmethyl]phenyl}acrylamide (26). 26 was synthesized from (*E*)-3-{4-[3-(2-phenyl-1*H*-indol-3-yl)piperidin-1-ylmethyl]phenyl}-acrylic acid methyl ester following general procedure D in 78% yield. <sup>1</sup>H NMR (400 MHz, CD<sub>3</sub>OD)  $\delta$  7.73 (d, *J* = 8.0 Hz, 1 H), 7.47 (m, 7 H), 7.35 (m, 4 H), 7.07 (t, *J* = 8.0 Hz, 1 H), 6.98 (t, *J* = 8.0 Hz, 1 H), 6.45 (d, *J* = 16 Hz, 1 H), 3.57 (dd, *J* = 16, 13 Hz, 2 H), 3.31 (m, 1 H), 2.94 (m, 2 H), 2.70 (t, *J* = 10 Hz, 1 H), 2.13 (m, 2 H), 1.90–1.68 (m, 3 H). Anal. RP-HPLC *t*<sub>R</sub> = 2.22 min (method 3, purity 100.00%/98.07%). HR-MS *m/z* (M + H)<sup>+</sup>: measd 452.2332, calcd 452.2338.

(*E*)-3-{4-[3-(2-*tert*-Butyl-1*H*-indol-3-yl)piperidin-1-ylmethyl]phenyl}-*N*-hydroxyacrylamide (27). 27 was synthesized from (*E*)-3-{4-[3-(2-*tert*-butyl-1*H*-indol-3-yl)piperidin-1-ylmethyl]phenyl}-acrylic acid methyl ester following general procedure D in

82% yield. <sup>1</sup>H NMR (400 MHz, CD<sub>3</sub>OD)  $\delta$  7.62 (d, *J* = 8.0 Hz, 2 H), 7.56 (m, 3 H), 7.45 (d, *J* = 8.0 Hz, 2 H), 7.31 (d, *J* = 8.0 Hz, 1 H), 6.99–6.89 (m, 2 H), 6.48 (d, *J* = 16 Hz, 1 H), 3.88 (br s, 2 H), 3.43 (m, 1 H), 3.18 (m, 1 H), 3.04 (m, 1 H), 2.53 (m, 1 H), 2.18 (m, 1 H), 1.95–1.82 (m, 4 H), 1.44 (s, 9 H). Anal. RP-HPLC *t*<sub>R</sub> = 3.11 min (method 1, purity 94.83%). HR-MS *m/z* (M + H)<sup>+</sup>: measd 432.2655, calcd 432.2651.

(*E*)-3-{3-Fluoro-4-[3-(1*H*-indol-3-yl)piperidin-1-ylmethyl]phenyl}-*N*-hydroxyacrylamide (28). 28 was synthesized from (*E*)-3-{4-[3-(1*H*-indol-3-yl)piperidin-1-ylmethyl]phenyl}-acrylic acid methyl ester following general procedure D in 9% yield. <sup>1</sup>H NMR (400 MHz, CD<sub>3</sub>OD)  $\delta$  7.54–7.45 (m, 3 H), 7.36–7.30 (m, 3 H), 7.06 (t, *J* = 8.0 Hz, 1 H), 7.01 (s, 1 H), 6.95 (t, *J* = 8.0 Hz, 1 H), 6.48 (d, *J* = 16 Hz, 1 H), 3.68 (s, 2 H), 3.17 (m, 2 H), 3.00 (m, 1 H), 2.22–2.02 (m, 3 H), 1.83 (m, 2 H), 1.55 (m, 1 H). Anal. RP-HPLC *t*<sub>R</sub> = 3.02 min (method 1, purity 100.00%). MS *m/z* 393.83 (M + H)<sup>+</sup>.

(*E*)-3-{3-Fluoro-4-[3-(2-phenyl-1*H*-indol-3-yl)piperidin-1-ylmethyl]phenyl}-*N*-hydroxyacrylamide (29). 29 was synthesized from (*E*)-3-{3-fluoro-4-[3-(2-phenyl-1*H*-indol-3-yl)piperidin-1-ylmethyl]phenyl}-acrylic acid methyl ester following general procedure D in 81% yield. <sup>1</sup>H NMR (400 MHz, CD<sub>3</sub>OD)  $\delta$  7.70 (d, *J* = 8.0 Hz, 1 H), 7.51–7.27 (m, 10 H), 7.07 (t, *J* = 8.0 Hz, 1 H), 6.97 (t, *J* = 8.0 Hz, 1 H), 6.47 (d, *J* = 16 Hz, 1 H), 3.65 (br s, 2 H), 2.96 (m, 2 H), 2.77 (t, *J* = 10 Hz, 1 H), 2.22 (m, 1 H), 2.08 (m, 1 H), 1.93–1.65 (m, 3 H), 1.33 (m, 1 H). Anal. RP-HPLC *t*<sub>R</sub> = 5.43 min (method 1, purity 100.00%). HR-MS *m/z* (M + H)<sup>+</sup>: measd 470.2226, calcd 470.2244.

(*E*)-3-{4-[3-(2-*tert*-Butyl-1*H*-indol-3-yl)piperidin-1-ylmethyl]-3-fluorophenyl}-*N*-hydroxyacrylamide (30). 30 was synthesized from (*E*)-3-{4-[3-(2-*tert*-butyl-1*H*-indol-3-yl)piperidin-1-ylmethyl]-3-fluorophenyl}-acrylic acid methyl ester following general procedure D in 11% yield. <sup>1</sup>H NMR (400 MHz, CD<sub>3</sub>OD)  $\delta$  7.56 (d, *J* = 8.0 Hz, 1 H), 7.50 (d, *J* = 16 Hz, 1 H), 7.41 (t, *J* = 8.0 Hz, 1 H), 7.28 (m, 4 H), 6.95 (t, *J* = 8.0 Hz, 1 H), 6.87 (t, *J* = 8.0 Hz, 1 H), 6.47 (d, *J* = 16 Hz, 1 H), 3.64 (br s, 2 H), 3.43 (m, 1 H), 3.01 (br d, *J* = 12 Hz, 1 H), 2.88 (m, 1 H), 2.75 (t, *J* = 12 Hz, 1 H), 2.21 (m, 1 H), 2.05 (m, 1 H), 1.79 (m, 3 H), 1.49 (s, 9 H). Anal. RP-HPLC *t*<sub>R</sub> = 2.90 min (method 3, purity 98.48%/95.39%). HR-MS *m/z* (M + H)<sup>+</sup>: measd 450.2559, calcd 450.2557.

(*E*)-3-{4-[3-(2-*tert*-Butyl-1*H*-indol-3-yl)piperidin-1-ylmethyl]-3-chlorophenyl}-*N*-hydroxyacrylamide (31). 31 was synthesized from (*E*)-3-{4-[3-(2-*tert*-butyl-1*H*-indol-3-yl)piperidin-1-ylmethyl]-3-chlorophenyl}-acrylic acid methyl ester following general procedure D in 53% yield. <sup>1</sup>H NMR (400 MHz, CD<sub>3</sub>OD)  $\delta$  7.65–7.47 (m, 5 H), 7.30 (d, *J* = 8.0 Hz, 1 H), 6.98–6.89 (m, 2 H), 6.48 (d, *J* = 16 Hz, 1 H), 3.81 (br s, 2 H), 3.48 (m, 1 H), 3.11 (m, 1 H), 2.94 (m, 2 H), 2.41 (m, 1 H), 2.15 (m, 1 H), 1.83 (m, 3 H), 1.43 (s, 9 H). Anal. RP-HPLC *t*<sub>R</sub> = 8.33 min (method 2, purity 100.00%/93.81%). HR-MS *m/z* (M + H)<sup>+</sup>: measd 466.2247, calcd 466.2261.

(*E*)-3-{4-[(*R*)-3-(2-*tert*-Butyl-1*H*-indol-3-yl)piperidin-1-ylmethyl]-3-fluorophenyl}-*N*-hydroxyacrylamide (32). 32 was synthesized from 2-*tert*-butyl-3-(*R*)-piperidin-3-yl-1*H*-indole following general procedures C and D in 45% yield. <sup>1</sup>H NMR (500 MHz, CD<sub>3</sub>OD)  $\delta$  7.59 (d, *J* = 10 Hz, 1 H), 7.49 (d, *J* = 15 Hz, 1 H), 7.46 (d, *J* = 10 Hz, 1 H), 7.32 (m, 4 H), 6.97 (t, *J* = 7.0 Hz, 1 H), 6.89 (t, *J* = 7.0 Hz, 1 H), 6.50 (d, *J* = 15 Hz, 1 H), 3.70 (br s, 2 H), 3.46 (m, 1 H), 3.05 (br d, *J* = 10 Hz, 1 H), 2.91 (br d, *J* = 10 Hz, 1 H), 2.79 (t, *J* = 10 Hz, 1 H), 2.26 (m, 1 H), 2.11 (m, 1 H), 1.82 (m, 3 H), 1.45 (s, 9 H). Anal. RP-HPLC *t*<sub>R</sub> = 9.36 min (method 2, purity 100.00%/96.46%). HR-MS *m/z* (M + H)<sup>+</sup>: measd 450.2565, calcd 450.2557.

(*E*)-3-{4-[(*S*)-3-(2-*tert*-Butyl-1*H*-indol-3-yl)piperidin-1-ylmethyl]-3-fluorophenyl}-*N*-hydroxyacrylamide (33). 33 was synthesized from 2-*tert*-butyl-3-(*S*)-piperidin-3-yl-1*H*-indole following general procedures C and D in 34% yield. <sup>1</sup>H NMR (500 MHz, CD<sub>3</sub>OD)  $\delta$  7.59 (d, *J* = 10.0 Hz, 1 H), 7.44 (d, *J* = 15 Hz, 1 H), 7.44 (t, *J* = 7 Hz, 1 H), 7.42 (d, *J* = 5.0 Hz, 1 H), 7.32 (d, *J* = 10 Hz, 2 H), 7.28 (d, *J* = 10 Hz, 1 H), 6.97 (t, *J* = 7 Hz, 1 H), 6.89 (t, *J* = 7 Hz, 1 H), 6.51 (d, *J* = 15 Hz, 1 H), 3.69 (br s, 2 H), 3.46 (m, 1 H), 3.05 (br d, *J* = 10 Hz, 1 H), 2.91 (br d, *J* = 10 Hz, 1 H), 2.79 (t, *J* = 10 Hz,

1 H), 2.25 (m, 1 H), 2.09 (m, 1 H), 1.82 (m, 3 H), 1.45 (s, 9 H). Anal. RP-HPLC  $t_R$  = 9.37 min (method 2, purity 95.69%/94.57%). HR-MS  $m/z$  (M + H)<sup>+</sup>: measd 450.2555, calcd 450.2557.

**Acknowledgment.** The authors thank Weijia Zheng for preparation of crystalline material for single-crystal X-ray analysis, Travis Stams for access to HDAC8 X-ray crystal structure, Robert Pearlstein for helpful advice on hERG modeling, and Karen Miller-Moslin, Christopher Brain, and Timothy Ramsey for helpful suggestions in the preparation of the manuscript.

**Supporting Information Available:** Figures A and B, Tables A and B, methods of automated Q-patch clamp studies, manual patch clamp electrophysiology and high-throughput determination of  $pK_a$ , procedure of NMR experiments for compound **30** and spectra, and X-ray structure data of (*S*)-3-(2-*tert*-butyl-1*H*-indol-3-yl)piperidine-1-carboxylic acid benzyl ester. This material is available free of charge via the Internet at <http://pubs.acs.org>.

## References

- Nightingale, K. P.; O'Neill, L. P.; Turner, B. M. Histone modifications: signaling receptors and potential elements of a heritable epigenetic code. *Curr. Opin. Genet. Dev.* **2006**, *16*, 125–136.
- Johnstone, R. W. Histone-deacetylase inhibitors: novel drugs for the treatment of cancer. *Nat. Rev. Drug Discovery* **2002**, *1*, 287–299.
- Bolden, J. E.; Peart, M. J.; Johnstone, R. W. Anticancer activities of histone deacetylase inhibitors. *Nat. Rev. Drug Discovery* **2006**, *5*, 769–784.
- de Ruijter, A. J. M.; van Gennip, A. H.; Caron, H. N.; Kemp, S.; van Kuilenburg, A. B. P. Histone deacetylases (HDACs): characterization of the classical HDAC family. *Biochem. J.* **2003**, *370*, 737–749.
- (a) Paris, M.; Porcelloni, M.; Binaschi, M.; Fattori, D. Histone deacetylase inhibitors: from bench to clinic. *J. Med. Chem.* **2008**, *51*, 1505–1529. (b) Miller, T. A.; Witter, D. J.; Belvedere, S. Histone deacetylase inhibitors. *J. Med. Chem.* **2003**, *46*, 5097–5116.
- Marks, P. A.; Breslow, R. Dimethyl sulfoxide to vorinostat: development of this histone deacetylase inhibitor as an anticancer drug. *Nat. Biotechnol.* **2007**, *25*, 84–90.
- Dokmanovic, M.; Clarke, C.; Marks, P. A. Histone deacetylase inhibitors: overview and perspectives. *Mol. Cancer Res.* **2007**, *5*, 981–989.
- Remiszewski, S. W.; Sambucetti, L. C.; Bair, K. W.; Bontempo, J.; Cesarz, D.; Chandramouli, N.; Chen, R.; Cheung, M.; Cornell-Kennon, S.; Dean, K.; Diamantidis, G.; France, D.; Green, M. A.; Howell, K. L.; Kashi, R.; Kwon, P.; Lassota, P.; Martin, M. S.; Mou, Y.; Perez, L. B.; Sharma, S.; Smith, T.; Sorensen, E.; Taplin, F.; Trogiani, N.; Versace, R.; Walker, H.; Weltchek-Engler, S.; Wood, A.; Wu, A.; Atadja, P.  $\alpha$ -Hydroxy-3-phenyl-2-propenamides as novel inhibitors of human histone deacetylase with in vivo antitumor activity: discovery of (2*E*)-*N*-hydroxy-3-[4-[(2-hydroxyethyl)[2-(1*H*-indol-3-yl)ethyl]amino]methyl]phenyl]-2-propenamide (NVP-LAQ824). *J. Med. Chem.* **2003**, *46*, 4609–4624.
- (a) Yurek-George, A.; Habens, F.; Brimmell, M.; Packham, G.; Ganesan, A. Total synthesis of spiruchostatin A, a potent histone deacetylase inhibitor. *J. Am. Chem. Soc.* **2004**, *126*, 1030–1031. (b) Crabb, S. J.; Howell, M.; Rogers, H.; Ishfaq, M.; Yurek-George, A.; Carey, K.; Pickering, B. M.; East, P.; Mitter, R.; Maeda, S.; Johnson, P. W. M.; Townsend, P.; Shin-ya, K.; Yoshida, M.; Ganesan, A.; Packham, G. Characterisation of the in vitro activity of the depsipeptide histone deacetylase inhibitor spiruchostatin A. *Biochem. Pharmacol.* **2008**, *76*, 463–475.
- (a) Furumai, R.; Matsuyama, A.; Kobashi, N.; Lee, K. H.; Nishiyama, N.; Makajima, I.; Tanaka, A.; Komatsu, Y.; Nishino, N.; Yoshida, M.; Horinouchi, S. FK228 (depsipeptide) as a natural prodrug that inhibits class I histone deacetylases. *Cancer Res.* **2002**, *62*, 4916–4921. (b) Bowers, A. A.; Greshock, T. J.; West, N.; Estiu, G.; Schreiber, S. L.; Wiest, O.; Williams, R. M.; Bradner, J. E. Synthesis and conformation–activity relationships of the peptide isosteres of FK228 and largazole. *J. Am. Chem. Soc.* **2009**, *131*, 2900–2905.
- (a) Jones, P.; Altamura, S.; Chakravarty, P. K.; Cecchetti, O.; De Francesco, R.; Gallinari, P.; Ingenito, R.; Meinke, P. T.; Petrocchi, A.; Rowley, M.; Scarpelli, R.; Serafini, S.; Steinkuehler, C. A series of novel, potent, and selective histone deacetylase inhibitors. *Bioorg. Med. Chem. Lett.* **2006**, *16*, 5948–5952. (b) Jones, P.; Altamura, S.; De Francesco, R.; Gonzalez Paz, O.; Kinzel, O.; Mesiti, G.; Monteagudo, E.; Pescatore, G.; Rowley, M.; Verdrame, M.; Steinkuehler, C. A novel series of potent and selective ketone histone deacetylase inhibitors with antitumor activity in vivo. *J. Med. Chem.* **2008**, *51*, 2350–2353.
- (a) Kranz, M.; Murray, P. J.; Taylor, S.; Upton, R. J.; Clegg, W.; Elsegood, M. R. J. Solution, solid phase and computational structures of apicidin and its backbone-reduced analogs. *J. Pept. Sci.* **2006**, *12*, 383–388. (b) The apicidin geometry was retrieved from the Cambridge Crystallographic Database, code number HEWGOG. Atomic coordinates were assumed to be at, or close to, a “global” minimum and subsequently held rigid in all calculations. Dacinostat conformations were generated as part of the alignment procedures used in FieldView. The aligned atomic coordinates of dacinostat in Figure 3 were inspected visually for strain and torsions using MOGUL (CCDC).
- (a) Nonpolar hydrogens were removed for a clear image. (b) *FieldAlign*; Cresset Biomolecular Discovery; Welwyn Garden City, U.K.
- A proprietary 2.1 Å resolution X-ray crystal structure of trichostatin A bound within HDAC8 was used as the template for generating an HDAC1 homology model using the PRIME software algorithm within the Maestro package from Schrodinger, Inc., of Portland, OR.
- Freter, K. 3-Cycloalkenylindoles. *J. Org. Chem.* **1975**, *40*, 2525–2529.
- Hénon, H.; Messaoudi, S.; Hugon, B.; Anizon, F.; Pfeiffer, B.; Prudhomme, M. Synthesis of granulatinamide bis-imide analogues. *Tetrahedron* **2005**, *61*, 5599–5614.
- Macor, J. E.; Chenard, B. L.; Post, R. J. Use of 2,5-dimethylpyrrole as an amino-protecting group in an efficient synthesis of 5-amino-3-[(*N*-methyl-pyrrolidine-2(*R*)-yl)methyl]indole. *J. Org. Chem.* **1994**, *59*, 7496–7498.
- Netherton, M. R.; Fu, G. C. Air-stable trialkylphosphonium salts: simple, practical, and versatile replacements for air-sensitive trialkylphosphines. Applications in stoichiometric and catalytic processes. *Org. Lett.* **2001**, *3*, 4295–4298.
- Rogers, C. J.; Dickerson, T. J.; Brogan, A. P.; Janda, K. D. Hammett correlation of nornicotine analogues in the aqueous aldol reaction: implications for green organocatalysis. *J. Org. Chem.* **2005**, *70*, 3705–3708.
- Cho, Y. S.; Jiang, L.; Shultz, M. Antitumor Heterocycle Compounds. Patent WO/2008/076954, 2008.
- (a) See Experimental Section. (b) See Figure A of Supporting Information for an induced-fit docking pose of dacinostat (7) docked within a hERG homology model. (c) See Supporting Information. (d) See Figure B of Supporting Information for induced-fit docking poses of **27** and **30** within a hERG homology model. (e) See Table A of Supporting Information. (f) See Table B of Supporting Information.
- (a) Cavalli, A.; Poluzzi, E.; De Ponti, F.; Recanatini, M. Toward a pharmacophore for drugs inducing the long QT syndrome: insights from a CoMFA study of hERG K<sup>+</sup> channel blockers. *J. Med. Chem.* **2002**, *45*, 3833–3853. (b) Aronov, A. M. Predictive in silico modeling for hERG channel blockers. *Drug Discovery Today* **2005**, *10*, 149–155. (c) Aronov, A. M. Tuning out of hERG. *Curr. Opin. Drug Discovery Dev.* **2008**, *11*, 128–135.
- Sanguinetti, M. C.; Tristani-Firouzi, M. hERG potassium channels and cardiac arrhythmia. *Nature* **2006**, *440*, 463–469.
- Farid, S.; Day, T.; Friesner, R. A.; Pearlstein, R. A. New insights about hERG blockade obtained from protein modeling, potential energy mapping, and docking studies. *Bioorg. Med. Chem.* **2006**, *14*, 3160–3173.
- Introduction of a hydrophilic substituent at C(2) of the indole resulted in loss of potency in both the enzyme and cellular assays and/or stronger inhibition of the hERG channel (data not shown).
- Böhm, H.-J.; Banner, D.; Bendels, S.; Kansy, M.; Kujn, B.; Müller, K.; Obst-Sander, U.; Stahl, M. Fluorine in medicinal chemistry. *Chem. Biol. Chem.* **2004**, *5*, 637–643.
- Computational experiments were performed on a Hewlett-Packard xw8200 workstation using the Red Hat Linux operating system, version 4.0. Spartan '08 for Windows (Wavefunction, Inc.) was used for construction of modeled structures and presenting the image for Figure 7a. Jaguar in the Maestro suite, version 8.5 (Schrodinger, Inc., Portland, OR), and Spartan '08 for Windows were used to perform density functional B3LYP calculations at the 6-31G\* level of theory in the gas phase. Because the *N*-hydroxyacrylamide moiety forms no close contacts with the ortho-fluoro or the piperidine nitrogen, this chemical fragment was removed from the molecular models as well as from subsequent calculations to increase computational speed while not compromising the experimental outcome.

- (28) (a) Francotte, E. Enantioselective chromatography as a powerful alternative for the preparation of drug enantiomers. *J. Chromatogr., A* **2001**, 906, 379–397. (b) Francotte, E. Isolation and Production of Optically Pure Drugs by Enantioselective Chromatography. In *Chirality in Drug Research*; Francotte, E., Lindner, W., Eds.; Methods and Principles in Medicinal Chemistry, Vol. 33; Wiley-VCH Verlag: Weinheim, Germany, 2006; Chapter 6. (c) Francotte, E.; Zhang, T. Photochemically Cross-Linked Polysaccharide Derivatives Having No Photopolymerisable Groups. Patent WO/1997/004011, 1997.
- (29) (a) Compound **32** was further profiled in the SCREENIT assay,<sup>29b–c</sup> an isolated rabbit heart preparation, to demonstrate the lack of proarrhythmogenic potential (no TRIaD: triangulation of the cardiac action potential, reverse use dependence, and instability) up to 3  $\mu$ M free plasma concentration ( $n = 3$ , 0.03, 0.1, 0.3, 1, and 3  $\mu$ M; the highest concentration tested was 3  $\mu$ M because of limited solubility of compound **32** in the assay conditions, although the high-throughput equilibrium solubility of an amorphous sample was measured as 0.042 mM at pH 6.8).<sup>21f</sup> In comparison, dacinostat (**7**) showed a proarrhythmic profile at  $\geq 2$   $\mu$ M ( $n = 6$ , delayed final repolarization phase (APD60 + triangulation)). (b) Hondeghem, L. M. Computer aided development of antiarrhythmic agents with class IIIa properties. *J. Cardiovasc. Electrophysiol.* **1994**, 5, 711–721. (c) Hondeghem, L. M.; Hoffmann, P. Blinded test in isolated female rabbit heart reliably identifies action potential duration prolongation and proarrhythmic drugs: importance of triangulation, reverse use dependence, and instability. *J. Cardiovasc. Pharmacol.* **2003**, 41, 14–24. (d) Valentin, J.-P.; Hoffmann, P.; De Clerck, F.; Hammond, T. G.; Hondeghem, L. M. Review of the predictive value of the Langendorff heart model (Screenit system) in assessing the proarrhythmic potential of drugs. *J. Pharmacol. Toxicol. Methods* **2004**, 49, 171–181. (e) Dumotier, B. M.; Deurinck, M.; Yang, Y.; Traebert, M.; Suter, W. Relevance of in vitro SCREENIT results for drug-induced QT interval prolongation in vivo: a database review and analysis. *Pharmacol. Ther.* **2008**, 119, 152–159.
- (30) (a) Gonzalez, T.; Arias, C.; Caballero, R.; Moreno, I.; Delpon, E.; Tamargo, J.; Valenzuela, C. Effects of levobupivacaine, ropivacaine and bupivacaine on HERG channels: stereoselective bupivacaine block. *Br. J. Pharmacol.* **2002**, 137, 1269–1279. (b) Yang, I. C.-H.; Scherz, M. W.; Bahinski, A.; Bennett, P. B.; Murray, K. T. Stereoselective interactions of the enantiomers of chromanol 293B with human voltage-gated potassium channels. *J. Pharmacol. Exp. Ther.* **2000**, 294, 955–962.
- (31) (a) The apparent discrepancy may be due to both the sensitivity limitation of the enzyme assay and the different assay durations. The enzyme assay measures the direct inhibition of compound on HDAC enzyme within 1 h of assay time, whereas the cellular proliferation assay measures the continuous compound effect over the course of 3 days which could lead to enhanced activity. (b) To ensure that the observed increase in the inhibition of cellular proliferation was based on improved HDAC inhibition and not a result of off-target activities, we screened **32** against over 60 GPCRs, enzymes, and transporters. Most of the IC<sub>50</sub> values are over 10  $\mu$ M, whereas the lowest IC<sub>50</sub> values are observed with histamine H2, cyclooxygenase 2, and adrenergic  $\alpha$ 1a receptor at 1–4  $\mu$ M, suggesting a relatively clean safety profile of **32**.